(12) INTERNATIONAL APPLICATION PUBLISHED UNDER THE PATENT COOPERATION TREATY (PCT)

(19) World Intellectual Property Organization
International Bureau

(43) International Publication Date
5 October 2006 (05.10.2006)

PCT

(10) International Publication Number
WO 2006/105094 A2

(51) International Patent Classification:
G01J 5/00 (2006.01)

(21) International Application Number:
PCT/US2006/011295

(22) International Filing Date: 29 March 2006 (29.03.2006)

(25) Filing Language: English

(26) Publication Language: English

(30) Priority Data:
60/665,837 29 March 2005 (29.03.2005) US

(71) Applicant *(for all designated States except US)*: **DUKE UNIVERSITY** [US/US]; Office of Science and Technology, P.O. Box 90083, Durham, NC 27708 (US).

(72) Inventors: **BRADY, David**; 2801 Dogwood Road, Durham, North Carolina 27705 (US). **GUENTHER, Bobby, D.**; 1002 Queensferry Road, Cary, NC 27511 (US). **FELLER, Steve**; 1007 N. Mangum Street, Durham, NC 27701 (US). **SHANKAR, Mohan**; 1200 Remington Circle, Durham, NC 27705 (US). **FANG, Jian-Shuen**; 1001 Iredell Street, Durham, NC 27705 (US). **HAO, Qi**; 2000 Baity Hill Drive, Apt. 123, Chapel Hill, NC 27514 (US).

(74) Agents: **GOTTS, Lawrence, J.** et al.; Pillsbury Winthrop Shaw Pittman LLP, 1650 Tysons Boulevard, P.O. Box 10500, McLean, VA 22102-4859 (US).

(81) Designated States *(unless otherwise indicated, for every kind of national protection available)*: AE, AG, AL, AM, AT, AU, AZ, BA, BB, BG, BR, BW, BY, BZ, CA, CH, CN, CO, CR, CU, CZ, DE, DK, DM, DZ, EC, EE, EG, ES, FI, GB, GD, GE, GH, GM, HR, HU, ID, IL, IN, IS, JP, KE, KG, KM, KN, KP, KR, KZ, LC, LK, LR, LS, LT, LU, LV, LY, MA, MD, MG, MK, MN, MW, MX, MZ, NA, NG, NI, NO, NZ, OM, PG, PH, PL, PT, RO, RU, SC, SD, SE, SG, SK, SL, SM, SY, TJ, TM, TN, TR, TT, TZ, UA, UG, US, UZ, VC, VN, YU, ZA, ZM, ZW.

(84) Designated States *(unless otherwise indicated, for every kind of regional protection available)*: ARIPO (BW, GH, GM, KE, LS, MW, MZ, NA, SD, SL, SZ, TZ, UG, ZM, ZW), Eurasian (AM, AZ, BY, KG, KZ, MD, RU, TJ, TM), European (AT, BE, BG, CH, CY, CZ, DE, DK, EE, ES, FI, FR, GB, GR, HU, IE, IS, IT, LT, LU, LV, MC, NL, PL, PT, RO, SE, SI, SK, TR), OAPI (BF, BJ, CF, CG, CI, CM, GA, GN, GQ, GW, ML, MR, NE, SN, TD, TG).

Published:
— *without international search report and to be republished upon receipt of that report*

For two-letter codes and other abbreviations, refer to the "Guidance Notes on Codes and Abbreviations" appearing at the beginning of each regular issue of the PCT Gazette.

(54) **Title:** SENSOR SYSTEM FOR IDENTIFYING AND TRACKING MOVEMENTS OF MULTIPLE SOURCES

(57) **Abstract:** One embodiment of the present invention is a system for identifying a human being from movement of the human being. The system includes a dual element pyroelectric detector, a Fresnel lens array, and a processor. The dual element pyroelectric detector detects radiation from the human being as the human being moves over time. The Fresnel lens array is located between the dual element pyroelectric detector and the human being. The Fresnel lens array improves collection efficiency and spatial resolution of the dual element pyroelectric detector. The Fresnel lens array includes a mask. The mask provides at least one zone of visibility. The processor is coupled to the dual element pyroelectric detector, the processor converts the detected radiation to a spectral radiation signature. The processor compares the spectral radiation signature to at least a second spectral radiation signature to identify the human being.

WO 2006/105094 A2

SENSOR SYSTEM FOR IDENTIFYING AND TRACKING MOVEMENTS OF MULTIPLE SOURCES

CROSS-REFERENCE TO RELATED APPLICATION

[0001] This application claims the benefit of U.S. Provisional Patent Application Serial No. 60/665,837 filed March 29, 2005, which is herein incorporated by reference in its entirety.

[0002] This invention was made with Government support under contract no. DAAD 19-03-1-03552 awarded by the Army Research Office. The Government has certain rights in the invention.

BACKGROUND OF THE INVENTION

FIELD OF THE INVENTION

[0003] Embodiments of the present invention relate to systems and methods for biometric tracking and authentication. More particularly, embodiments of the present invention relate to systems and methods for identifying and authenticating human motion using radiation detectors.

BACKGROUND INFORMATION

[0004] Biometric systems are widely used in person metrication and secure identification. Some of the biometric systems implemented include fingerprint scanners, iris or retina scanners, pressure pads, face recognition, and voice recognition. All of these implementations use high resolution/high sensitivity devices making them unscalable in terms of bandwidth, computation cost, or both.

[0005] In view of the foregoing, it can be appreciated that a substantial need exists for systems and methods that can advantageously provide for scalable and low cost biometric tracking and authentication.

BRIEF SUMMARY OF THE INVENTION

[0006] One embodiment of the present invention is a system for identifying an object from movement of the object. The system includes a sensor and a processor. The sensor detects radiation from the object as the object moves over time. The processor is coupled to the sensor. The processor converts the detected radiation to a spectral radiation signature. The processor compares the spectral radiation signature to at least a second spectral radiation signature to identify the object.

[0007] Another embodiment of the present invention is a system for identifying an object from movement of the object. The system includes a sensor and a

processor. The sensor detects radiation from the object as the object moves along a first path over time. The processor is coupled to the sensor. The processor converts the detected radiation to a spectral radiation signature. The processor obtains temporal radiation data from a second object moving along a second path using the sensor. The processor converts the temporal radiation data from the second object to a second spectral radiation signature. The processor applies principal components analysis to the second spectral radiation signature to produce underlying factors and scores for the second spectral radiation signature. The processor applies a multiple linear regression to the underlying factors and scores to produce a regression vector and a mean and covariance of clustered data for the second spectral radiation signature. The processor obtains an inner product of the regression vector and the spectral radiation signature. The processor compares the inner product to the mean and covariance of clustered data to determine if the identity of the object matches the second object.

[0008] Another embodiment of the present invention is a method for identifying an object from movement of the object. First temporal radiation data is obtained from a first object moving along a first path using the sensor. The first temporal radiation data from the first object is converted to a first spectral radiation signature. Principal components analysis is applied to the first spectral radiation signature to produce underlying factors and scores for the first spectral radiation signature. Multiple linear regression is applied to the underlying factors and scores to produce a regression vector and a mean and covariance of clustered data for the first spectral radiation signature. Second temporal radiation data is obtained from a second object moving along a second path using the sensor. The second temporal radiation data from the second object is converted to a second spectral radiation signature. An inner product of the regression vector and the second spectral radiation signature is calculated. The inner product is compared to the mean and covariance of clustered data to determine if the identity and location of the first object match the second object.

[0009] Another embodiment of the present invention is a system for identifying a human being from movement of the human being. The system includes a dual element pyroelectric detector, a Fresnel lens array, and a processor. The dual element pyroelectric detector detects radiation from the human being as the human being moves over time. The Fresnel lens array is located between the dual

element pyroelectric detector and the human being. The Fresnel lens array improves collection efficiency and spatial resolution of the dual element pyroelectric detector. The Fresnel lens array includes a mask. The mask provides at least one zone of visibility. The processor is coupled to the dual element pyroelectric detector, the processor converts the detected radiation to a spectral radiation signature. The processor compares the spectral radiation signature to at least a second spectral radiation signature to identify the human being.

[0010] Another embodiment of the present invention is a system for identifying a human being from movement of the human being. The system includes a dual element pyroelectric detector, a Fresnel lens array, and a processor. The dual element pyroelectric detector detects radiation from the human being as the human being moves along a first path over time. The Fresnel lens array is located between the dual element pyroelectric detector and the human being. The Fresnel lens array improves collection efficiency and spatial resolution of the dual element pyroelectric detector. The Fresnel lens array includes a mask. The mask provides at least one zone of visibility. The processor is coupled to the dual element pyroelectric detector, the processor converts the detected radiation to a spectral radiation signature. The processor obtains temporal radiation data from a second human being moving along a second path using the sensor. The processor converts the temporal radiation data from the second human being to a second spectral radiation signature. The processor applies principal components analysis to the second spectral radiation signature to produce underlying factors and scores for the second spectral radiation signature. The processor applies a multiple linear regression to the underlying factors and scores to produce a regression vector and a mean and covariance of clustered data for the second spectral radiation signature. The processor obtains an inner product of the regression vector and the spectral radiation signature. The processor compares the inner product to the mean and covariance of clustered data to determine if the identity of the human being matches the second human being.

BRIEF DESCRIPTION OF THE DRAWINGS

[0011] Figure 1 is an exemplary plot of a black-body radiation curve of a human body at 37 degrees Celsius, in accordance with an embodiment of the present invention.

[0012] Figure 2 is a schematic diagram of a sensor system for identifying and tracking movement of an object, in accordance with an embodiment of the present invention.

[0013] Figure 3 is an exemplary polar plot of a dual element pyroelectric detector response, in accordance with an embodiment of the present invention.

[0014] Figure 4 is schematic diagram of a pyroelectric sensor, in accordance with an embodiment of the present invention.

[0015] Figure 5 is an exemplary top view of a field of view of a Fresnel lens array, in accordance with an embodiment of the present invention.

[0016] Figure 6 is an exemplary side view of a field of view of a Fresnel lens array, in accordance with an embodiment of the present invention.

[0017] Figure 7 is a schematic diagram of four plastic masks for Fresnel lens arrays containing one, three, five, and seven elements, in accordance with an embodiment of the present invention.

[0018] Figure 8 is a flowchart of an identification method of a sensor system for identifying and tracking movement of an object, in accordance with an embodiment of the present invention.

[0019] Figure 9 is an exemplary plot of temporal voltage signals generated by a human walking across the field of view of a pyroelectric sensor, in accordance with an embodiment of the present invention.

[0020] Figure 10 is an exemplary plot of a spectra corresponding to voltage signals generated by a human walking across the field of view of a pyroelectric sensor, in accordance with an embodiment of the present invention.

[0021] Figure 11 is an exemplary plot of supervised clustering results upon six labels for 120 data sets collected from a pyroelectric sensor including an eleven-element Fresnel lens array, in accordance with an embodiment of the present invention.

[0022] Figure 12 is an exemplary plot of probability density distribution of the clusters shown in Figure 11, in accordance with an embodiment of the present invention.

[0023] Figure 13 is an exemplary plot of identification results for a sensor unit with an eleven-element lens array at a sensor object distance of two meters and a sensor unit placed at a height of 80 centimeters, in accordance with an embodiment of the present invention.

[0024] Embodiments of the invention are described in detail below. One skilled in the art, however, will appreciate that the invention is not limited in its application to the details of construction, the arrangements of components, and the specific steps set forth in the detailed description or illustrated in the drawings. The invention is capable of other embodiments and of being practiced or being carried out in various ways. Also, it is to be understood that the phraseology and terminology used herein is for the purpose of description and should not be regarded as limiting.

BRIEF DESCRIPTION OF THE APPENDICES

[0025] Appendix 1 is a description of a sensor system used to identify and track human motion, in accordance with an embodiment of the present invention.

DETAILED DESCRIPTION OF THE INVENTION

[0026] The present invention is based upon the radiation characteristics of an object, such as a person, animal, or vehicle. The temperature of a typical human body is about 37 degrees C or 98 degrees F. There is a constant heat exchange between the body and the environment due to the difference in their temperatures. The radiation characteristics of any object can be analyzed using the black-body radiation curve governed by Planck's Law.

[0027] Figure 1 is an exemplary plot 100 of a black-body radiation curve 110 of a human body at 37 degrees Celsius, in accordance with an embodiment of the present invention. In Figure 1, it can be seen that essentially all of the radiation is in the infrared region, with the peak radiation occurring at 9.55 μm. To estimate human body radiation of heat to its environment, Planck's Law is integrated over the transmission window of a sensor. The average human body radiates about 100 W/m^2 of power. Thus, infrared detectors that are sensitive in a range of 8~14 μm are able to detect humans within a reasonable distance.

[0028] A pyroelectric infrared (PIR) sensor has high performance for infrared (IR) radiation detection at room temperature. Recently, PIR sensors have been used for a wide range of applications such as intruder detection, light actuators, and auxiliary sensing to complement the coverage of cameras. PIR sensors are attractive for security applications due to their low cost and low power consumption. Equally attractive, PIR sensors do not need special or expensive cooling.

[0029] According to another embodiment of the present invention, a wireless distributed pyroelectric sensor system is used for human target tracking. One aspect of human tracking is human identification or recognition. Human identification not only plays an important role in security systems and scene surveillance, but also is a necessity for tracking multiple humans, by reducing the mutual interference among those human objects during the tracking process.

[0030] According to another embodiment of the present invention, a pyroelectric sensor system for human recognition serves as a component of a biometric system, a requirement for many intelligent machine systems and secure systems. In conventional biometric systems, the complex structure of certain body parts, such as a human iris, human fingerprints, facial, or hand geometry, are measured optically, analyzed digitally, and a digital code is created for each person. When humans walk, the motion of various components of the body, including the torso, arms, and legs, produce a characteristic signature.

[0031] According to another embodiment of the present invention, a pyroelectric sensor system detects the motion of various components of the body, including the torso, arms, and legs, and produces a characteristic signature that it is sufficiently discriminatory to allow verification in some low-security applications. Much of the work on gait analysis as a behavior biometric has been conducted using video cameras which stream and process large amounts of data to extract the identity of the person under examination in a computationally expensive way. A continuous-wave (CW) radar, for example, has been developed to record the radar signature corresponding to the walking human gait.

[0032] From a thermal perspective, each person acts as a distributed infrared source whose distribution function is determined by their shape and the IR emission of their extremity. Combined with the idiosyncrasies in how they carry themselves, the heat impacts a surrounding sensor field in a unique way. By measuring the sensor response to a person in a prescribed walking path, this response data is mapped to a code vector in a two-dimensional (2-D) plane that uniquely identifies the person at a specific speed level.

[0033] A functional biometric system requires the specific human characteristics in use to be universal, distinctive, permanent, and collectable. Universal means each person should have his/her own characteristic. Distinctive means any two persons should have separable characteristics. Permanent means the characteristic

should be sufficiently invariant, under a certain matching criterion, over a period of time. Collectable means the characteristic must be a measurable quantity. A biometric system is an intrinsic pattern recognition system and comprises three parts: feature representation, feature training (clustering), and feature testing.

[0034] According to another embodiment of the present invention, data collected from a sensor (*e.g.*, a pyroelectric sensor) is analyzed using spectral techniques to extract the motion features of individuals. The experimental results display the spectral distinctions among different humans walking at different speeds. The spectral features of objects at a specific speed are collected repeatedly with small variances, given a fixed sensor configuration. By using a principal component regression (PCR) method, those spectral features are clustered around a set of points, along a unit circle in a 2-D label plane. From the training process, a regression vector locating a cluster is obtained, as well as the mean and covariance of a number of clusters. Then new data, of persons walking at random speeds, are used for testing the recognition capability.

[0035] Figure 2 is a schematic diagram of a sensor system 200 for identifying and tracking movement of a person 240, in accordance with an embodiment of the present invention. System 200 includes sensor 210 and processor 220. Sensor 210 can include but is not limited to one or more lenses, coded apertures, programmable amplifiers, and radiation detectors. Sensor 210 is mounted on pillar 230 at height 270. Sensor 210 detects radiation from person 240 as person 240 moves past sensor 210 along path 250. Distance 260 is the perpendicular distance between pillar 230 and path 250. Processor 220 is coupled to sensor 210.

[0036] According to another embodiment of the present invention, data from sensor 210 is collected into a packet and transmitted by an attached half-duplex wireless transmitter, a TRF6901 for example, to a similarly constructed collection node, where it undergoes additional signal processing and is relayed by a serial interface to processor 220 for analysis and display. A standard communication protocol is used in the transmission of data between each of the nodes and the master node along with error correction mechanisms for each transmitted byte. The wireless transmitters preferably operate at 20Kkps (kilobits per second) and can be programmed to use variable frequencies. Making each node use its own frequency and performing frequency hopping on the collection nodes minimizes the communication protocol requirements while maximizing data throughput.

[0037] Processor 220 is used to process the information from sensor 210 in order to identify and track person 240. Person 240 can also be but is not limited to a vehicle or an animal. Person 240 is an object that radiates energy, for example, heat. Processor 220 creates a heat signature of person 240 from the measurements of sensor 210 and discriminates between different objects by comparing their heat signatures. Parameters that impact the identification performance of processor 220 include but are not limited to characteristics of a coded aperture, height 270, and distance 260.

[0038] PIR detectors are advantageous for use in sensor 210, because of their low cost and low power consumption. A PIR detector costs $2, for example. A PIR detector consumes 2 mW, for example. PIR detectors are available in single element or dual element versions. A single element detector responds to any temperature changes in the environment and therefore needs to be thermally compensated to remove sensitivity to ambient temperature. Dual element detectors have the inherent advantage that the output voltage is the difference between the voltages obtained from each of the elements of the detector, which subtracts out environmental effect.

[0039] Figure 3 is an exemplary polar plot 300 of a dual element pyroelectric detector response 310, in accordance with an embodiment of the present invention. Response 310 is toward a point source, where the distance between the point source under testing and the sensor is normalized to show its generic visibility characteristic. A dual lobe visibility pattern is formed because the two pyroelectric elements are connected in series opposition. The signals obtained from each of the elements where a thermal source crosses the common area of overlap of the fields of view (FOVs) cancel one another.

[0040] An exemplary dual element pyroelectric detector is the PIR325 from Glolab Corporation. This detector can be used to detect IR radiation from human bodies. Each element of the detector has an angular visibility of over 100 degrees, but any motion near both the margins of the FOV does not create a significant change in the thermal flux, resulting in very little response. The response of the detector depends on the incident power collected by the detector which in turn depends on the area of the detector. Since the detector elements have a small area

($2\ mm^2$), the amount of power collected is a very small fraction of the incident power.

[0041] Pyroelectric detectors in themselves do not shed much light on the nature of the heat source they observe, because their resolution and collection efficiency are poor. Coded apertures are used as a visibility modulating element. The space is segmented and encoded based on the number of detectors and each spatial region is assigned a unique combination of overlapping detectors. A reference structure mask is then designed to modulate the visibility of the sensors to implement this code. A problem with coded apertures is that the signal to noise ratio (SNR) is poor, since much of the incident radiation is blocked by the mask.

[0042] According to another embodiment of the present invention, to improve both the collection efficiency and spatial resolution, Fresnel lens arrays are used to create a discontinuous visibility pattern. These sensors, therefore, trigger as heat sources cross the boundaries created by the visibility pattern. The nature of a lens array allows the visibility space to be segmented into multiple boundaries.

[0043] Fresnel lenses are very good energy collectors, and have been used extensively in non-imaging applications. They are especially useful for IR applications because of low fabrication costs and good transmission characteristics in the infrared.

[0044] Figure 4 is schematic diagram of a pyroelectric sensor 400, in accordance with an embodiment of the present invention. Pyroelectric sensor 400 includes lens aperture 410 and dual element pyroelectric detector 420. Lens aperture 410 is used to improve both the collection efficiency and spatial resolution of dual element pyroelectric detector 420. Lens aperture 410 can be but is not limited to a Fresnel lens. A Fresnel lens can be molded out of inexpensive plastics with desired transmission characteristics (for the required wavelength range) making pyroelectric sensor 400 thin, light weight, and inexpensive.

[0045] In order to aid in motion sensing, Fresnel lens arrays are designed so that the visible space is divided into zones. Detection is enhanced by creating distinct regions of visibility. Each of the lenses on the array would typically create a single cone of visibility depending on the focal length and the size of the detector elements. However, with dual element pyroelectric detector 420, the cone of visibility of a lens is divided into two distinct zones, as illustrated in Figure 4.

[0046] Figure 5 is an exemplary top view 500 of a field of view of a Fresnel lens array, in accordance with an embodiment of the present invention. Each lens on the array produces two beams having an angular visibility. Visibility angle 510 is 3 degrees, for example, separated by angle 520, which is 1 degree, for example.

[0047] Figure 6 is an exemplary side view 600 of a field of view of a Fresnel lens array, in accordance with an embodiment of the present invention. Visibility angle 610 is 12 degrees, for example. An exemplary Fresnel lens array is the "Animal alley array- AA0.9GIT1" from Fresnel Technologies, Inc. The material of this lens has suitable transmission in the 8-14 μm range. A summary of the different parameters of this lens array is shown in Table 1 below.

Parameter	Value
Angular coverage of each lens	7°
Angular gap between adjacent beams	2°
Angular gap between two beams from each lens	1°
Lateral angular spread	12°
Transmittance of lens in IR	75 %

Table 1

[0048] Figure 7 is a schematic diagram of four plastic masks 700 for Fresnel lens arrays containing one, three, five, and seven elements or visibility zones, in accordance with an embodiment of the present invention. Fresnel lens arrays are available with a number different elements. For example, Fresnel lens arrays are available with 1, 3, 5, 7, 9, and 11 elements.

[0049] A wide variety of tracking methodologies such as Bayesian statistics can be applied to the tracking problem and within the particular statistics used, a number of strategies such as Kalman, Gaussian particle filters, and Hidden Markov Model. Tracking methodologies are further described in Appendix 1. The tracking methodology selected is driven by the amount of on-board processing power available. The Fresnel lens can shape the visibilities of pyroelectric sensors to detection regions with different visibility patterns and when humans enter different regions, different sets of sensors can fire simultaneously, and from those signal patterns the locations of people can be obtained.

[0050] Humans move in generally the same way, but with subtleties that can be recognized by those who are familiar with them, even at a distance. The multiplex nature of pyroelectric sensors allow capture of relatively small amounts of data that still bear the unique aspects of a person's movement. Because the pyroelectric sensors collectively project a set of boundary planes that cut through the intervening space, the subtle aspects of a person's gait will directly affect the sensors measurement.

[0051] Discrimination between members of a group are made by collecting data generated by the pyroelectric system such as the spectral content of the sensor's temporal signal, generated by humans walking along a path. During a training phase, features are collected and used to discriminate between registered humans while rejecting unregistered humans.

[0052] Figure 8 is a flowchart of an identification method 800 of a sensor system for identifying and tracking movement of an object, in accordance with an embodiment of the present invention. System 800 includes both training and testing paths.

[0053] In step 805 of method 800, temporal data of an object moving along a first path is obtained from a pyroelectric sensor. This is temporal training data.

[0054] In step 810, temporal training data is converted to a spectral radiation signature. A fast fourier transform (FFT) is used to create a Fourier spectra, for example. The result is spectral training data.

[0055] In step 815, a smoothing function is applied to the spectral training data to reduce noise present in the signal.

[0056] In step 820, principal components analysis is applied to the spectral training data. The results are the underlying factors and their scores for the spectral training data. Principal components analysis identifies significant spectral components from the Fourier spectra of the training data. A significant spectral component for a person walking can be but is not limited to the swinging of an arm or leg, the bobbing of the head, or the velocity of the person's body. These spectral components are the underlying factors and scores provided by principal components analysis. Discrete values for the underlying factors and scores are obtained by sampling the spectral components, for example. A matrix of discrete values for the underlying factors and score is produced from multiple data sets of training data from the same object.

[0057] In step 825, multiple linear regression is applied to the underlying factors and their scores to regress those scores. The result is a regression vector for training data and a mean and covariance of clustered training data. Multiple linear regression is used to reduce multiple lists (*e.g.*, a matrix) of spectral components obtained from multiple samples of training data to a single list (*e.g.*, a vector) of spectral components that uniquely identify the movement of the object. Multiple linear regression also provides a mean and covariance for each spectral component from the multiple lists or data sets.

[0058] In step 830, temporal data of an object moving along a second path is obtained from a pyroelectric sensor. This is temporal testing data.

[0059] In step 835, temporal testing data is converted to spectral radiation signature. A Fast Fourier transform is used to create a Fourier spectra, for example. The result is spectral testing data.

[0060] In step 840, a smoothing function is applied to the spectral testing data to reduce noise present in the signal.

[0061] In step 845, the inner product of the regression vector and the spectral testing data is obtained. The result is an estimate of the identity of a spectrum of the testing data. Like the training data, the spectral testing data also consists of more than one data set in order to reduce the effects of noise. As a result, there are multiple spectrums for the testing data. These multiple spectrums are represented in discrete form, for example, by a matrix. The inner product of this matrix and the regression vector is then used to produce an identity vector.

[0062] In step 850, the estimated identity of the spectrum of the testing data is checked against the clustered data of the training process and identified and unidentified objects are found. These identified and unidentified objects are also called registered and unregistered objects, respectively. An identified or registered object is one whose estimated identity of the spectrum is within a certain threshold of an object previously detected in the training phase. The threshold is selected by analyzing large sets of data. The threshold determines the accuracy of the system.

[0063] The first path of step 805 is, for example, a fixed or known path and the second path of step 830 is an unknown path. In another embodiment of the present invention, a senor array, or multiple sensor nodes, and additional feature representations are employed to improve the robustness of the system. With more

advanced signal processing and feature extraction techniques, for example, the first path of step 805 does not need to be fixed or known. The result is a path-independent human recognition system, which is also less sensitive to the walking speed of objects.

[0064] Mathematically, PCR is used to find a regression vector F, such that the identity of a spectrum of unknown sensory data can be estimated, by an inner product of vector F and the spectrum *S*.

$$I = S \bullet F . \tag{1}$$

[0065] PCR uses the full spectrum, and is factor-based. The spectral information is not directly used in training, but is subject to factor analysis to find those factors that have the largest influence on data variations. PCR is divided into two steps: principal components analysis (PCA) followed by standard multiple linear regression (MLR). In multiple hypothesis testing (MHT), the identity of an unknown spectrum is estimated by Eq. (1) and then is checked against clusters and their distributions obtained from the training process.

[0066] PCA is a spectral decomposition of the spectrum matrix S, retaining only those factors that have large singular values. The remaining factors associated with small singular values are assumed to be from noise, and therefore omitted from the later regression phase. The singular value decomposition (SVD) of a spectral matrix S can be represented by the following equation.

$$S_{m\times n} = U_{m\times m}\Sigma_{m\times n}V^T_{n\times n} , \tag{2}$$

U and V are orthogonal matrices, m is the number of samples, n is the number of spectral points in one spectrum of the sensor's temporal signal.

$$\Sigma = \begin{bmatrix} \sigma_1 & & & & & & \\ & \sigma_2 & & & & & \\ & & \cdots & & & & \\ & & & \sigma_r & & & \\ & & & & 0 & & \\ & & & & & \cdots & \\ & & & & & & \cdots \\ & & & & & & 0 \end{bmatrix} . \tag{3}$$

Σ is diagonal with nonnegative singular values in descending order. Thus the spectrum matrix S can also be written as,

$$S = \sum_{i=1}^{r} \sigma_i u_i v_i^T = \sigma_1 u_1 v_1^T + \sigma_2 u_2 v_2^T + \ldots + \sigma_r u_r v_r^T . \tag{4}$$

S can be approximated by its first k singular values, assuming singular values for larger k are negligible.

$$S \approx S_k = \sum_{i=1}^{k} \sigma_i u_i v_i^T \qquad (5)$$

$$= \sigma_1 u_1 v_1^T + \sigma_2 u_2 v_2^T \ldots + \sigma_k u_k v_k^T$$

$$= \tilde{U}_{m\times k} \tilde{\Sigma}_{k\times k} \tilde{V}_{k\times n},$$

where $k << m,n$.

[0067] The spectrum matrix S also can be defined as

$$S \approx TP^T, \qquad (6)$$

where

$$T_{m\times k} = \tilde{U}_{m\times k} \tilde{\Sigma}_{k\times k},$$

$$P = \tilde{V}_{k\times n},$$

$$SP = T.$$

[0068] T is the score matrix, and P is the factor matrix. Geometrically, P is viewed as a new set of orthogonal coordinates spanning the inherent (true) dimensionality of the spectrum data matrix S, and T is the projection (scores) of S onto new coordinate system. It is called k-space.

[0069] Once underlying factors and their corresponding scores are obtained, MLR is performed to regress those scores. In the classification process, the Fourier spectrum is first projected onto those factors obtained during training, and the resulting scores are correlated with the calibration vector obtained by MLR in k-space. The spectrum vector is regressed against the score matrix $T_{m\times k}$, to get the regression vector $f_{k\times 1}$ in k-space. For example, the least-squares solution of the following equation is found.

$$I_{m\times 1} = T_{m\times k} f_{k\times 1}. \qquad (7)$$

The least-squares solution for $f_{k\times 1}$ is

$$f_{k\times 1} = (T^T T)^{-1} T^T I = \tilde{\Sigma}^{-2} T^T I, \qquad (8)$$

where

$$\tilde{\Sigma}^{-2} = \begin{bmatrix} \frac{1}{\sigma_1^2} & & & \\ & \frac{1}{\sigma_2^2} & & \\ & & \cdots & \\ & & & \frac{1}{\sigma_k^2} \end{bmatrix} \tag{9}$$

Finally, from Eq. (6), Eq. (7), and Eq. (8) the regression vector can be written as follows.

$$\begin{aligned} F_{n\times 1} &= P_{n\times k} f_{k\times 1} \\ &= P_{n\times k} (\tilde{\Sigma})^{-2} (T)^T I \\ &= \tilde{V}_{n\times k} (\tilde{\Sigma})^{-2} (\tilde{U}_{m\times k} \tilde{\Sigma}_{k\times k})^T I \\ &= \tilde{V}_{n\times k} (\tilde{\Sigma})^{-1} (\tilde{U}_{m\times k})^T I \end{aligned} \tag{10}$$

[0070] From multiple linear regression, the resultant regression vector is obtained, as well as mean and covariance of clustered training data, $[\mu_1, \ldots, \mu_K]$ and $[\Sigma_1, \ldots, \Sigma_K]$, where K is the number of clusters. Therefore, for an unlabeled spectrum x, there are K+1 hypothesis, $\{H_0, H_1, \ldots, H_K\}$, to test. The hypothesis H_0 represents "none." The decision rule then is

$$x \in \begin{cases} H_0, & \text{if } \max_i \{p(x \mid H_i)\} < \gamma \\ H_i: \ i = \arg\max_i \{p(x \mid H_i)\}, & \text{otherwise} \end{cases} \tag{11}$$

where $p(x|H_i) = N(x|\mu_i, \Sigma_i)$ is the association of x with the i^{th} cluster and γ is a selected rejection threshold. Recognition ability of the process is measured by the false alarm rate, which can be defined by the following equation.

$$FAR = \frac{\#\ of\ false\ sets}{\#\ of\ testing\ sets}$$

[0071] According to another embodiment of the present invention, experimental data is collected using pyroelectric system 200 of Figure 2. Sensor 210 includes a PIR detector and a Fresnel lens array. Sensory data is collected when difference people walk back and forth along a prescribed straight path 250, where distance 260 is between two and three meters. Height 270 is approximately 80 centimeters. Data is collected as a human 240 moves along path 250.

[0072] In response to heat flow, electric charge is built up on a pyroelectric detector of sensor 210 by virtue of its pyroelectric property. The electric charge

results in an electric current which is converted to a voltage signal by a current to voltage amplifier (*e.g.*, a transductance amplifier).

[0073] Figure 9 is an exemplary plot 900 of a temporal voltage signal 910 generated by a human walking across the field of view of a pyroelectric sensor, in accordance with an embodiment of the present invention.

[0074] Figure 10 is an exemplary plot 1000 of a spectra 1010 corresponding to voltage signals generated by a human walking across the field of view of a pyroelectric sensor, in accordance with an embodiment of the present invention.

[0075] The Fourier spectra generated by two people walking at a similar speed are generally different. Also, for the same person, different speeds produce spectral differences. Hence, in addition, the effects of speed are taken into account in building a functional identification system.

[0076] According to another embodiment of the present invention, an optimal number of elements of a Fresnel lens array is found by modulating the visibility of pyroelectric sensors by Fresnel lens arrays with 1, 3, 5, and 11 transparent elements. Exemplary masks used for selection of different lens elements are shown in Figure 7.

[0077] According to another embodiment of the present invention, the effects of the sensor location and sensor-target distance upon the identification performance are studied. The sensor unit is located at the heights of 35cm, 80cm, and 120cm respectively and two fixed-paths, 2 m and 3 m, from the sensor are used. For each sensor-object configuration, 60 sets of data are collected for each person walking back and forth along a fixed-path at 3 different speed levels, namely fast, moderate, and slow, all within the range of the daily walking habit. The Fourier spectra of measured signals of the two human objects are collected. Data collected at the different walking speeds is displayed in columns. Data obtained with the different element numbers of Fresnel lens arrays is displayed in rows. Each plot contains 20 superimposed data sets which are gathered from 20 independent walks. By reviewing such displays it is seen that there is a degree of spectra overlap and that the repeatability of the spectral features is high.

[0078] According to another embodiment of the present invention, an identification procedure consists of two parts: training and testing. During training, 120 data sets are clustered from each sensor-lens pair into 6 clusters, two persons, and three speeds. Since the label of each data set is known, the clustering

process is viewed as supervised training. As such, these 6 clusters are mapped to 6 points equally distributed along a circle using linear regression. The resultant regression vector obtained from PCR defines the linear boundary between the data sets.

[0079] Figure 11 is an exemplary plot 1100 of supervised clustering results upon six labels for 120 data sets collected from a pyroelectric sensor including an eleven-element Fresnel lens array, in accordance with an embodiment of the present invention. The six circles 1110 represent the locations of clustered results for two different people walking at three different speeds. Each circle 1110 is then surrounded by 20 data points that represent 20 separate walks by a particular person at a particular speed. The data points are placed on plot 1100, for example, based on the relative locations of two spectral components. Diamonds 1120 are, for example, 20 walks by Jason at slow speed, while stars 1130 are 20 walks by Bob at a fast speed. Figure 11 shows that both different people and the speed of movement of the same person can be distinguished by an embodiment of the present invention.

[0080] Clustering results are obtained for the sensor units with 1, 5, and 11-element Fresnel lens arrays. The results show that the use of an increased number of lens elements in the lens array yield better performance in the supervised classification.

[0081] Figure 12 is an exemplary plot 1200 of probability density distributions of the clusters shown in Figure 11, in accordance with an embodiment of the present invention. Figure 12 shows the contours 1210 of probability density distributions (pdfs) associated with the clusters in Figure 11. Contours 1210 of probability density ranging from 0.1 to 0.7 are drawn in Figure 12 to aid in interpretation. These contours are used to specify a threshold that determines whether or not an object has been identified.

[0082] According to another embodiment of the present invention, after determining the optimal number of lens element, the effects of sensor locations are studied. Clustering results and their pdfs are obtained for the sensor unit with an 11-element lens array placed at the heights of 120 cm and 35 cm, respectively.

[0083] According to another embodiment of the present invention, MHT is carried out for human identification. 20 data sets are collected for each person walking at random speeds. For two registered persons, there are 40 data sets for

each configuration of sensor units. A probability density of each data set is calculated to determine its cluster membership. The threshold for membership is chosen to be 0.05. If the probability density value of a data set is below the threshold, the data set is labeled as others.

[0084] Figure 13 is an exemplary plot 1300 of identification results for a sensor unit with an eleven-element lens array at the a sensor object distance of two meters and a sensor unit placed at a height of 80 centimeters, in accordance with an embodiment of the present invention. False data sets 1310 are, for example, used to calculate a false alarm rate.

[0085] Results similar to Figure 13 are obtained for the sensor unit with an eleven-element Fresnel lens array at a total of three different heights and at a total of two different distances from the object using four different Fresnel lens arrays. Data is generated for two objects: Bob and Jason.

[0086] The false alarm rates for different sensor configurations and for a single person are summarized below in Table 2. For example, the false alarm rate for Bob walking along a path 3 m (*L*) from a pillar on which an eleven-element (*N*) sensor is mounted 80 cm (*H*) above the ground is 2.5 %. In other words, a system as shown in Figure 2, where the path is 3 m from the pillar and the sensor includes an eleven-element sensor mounted 80 cm above the ground can identify Bob from other people 97.5 % of the time. The false alarm rate was defined earlier. It can be seen that the sensor unit with an 11-element lens array located at the height of 80 cm displays the best performance.

H	**35 cm**		**80 cm**		**120 cm**	
L / *N*	**2 m**	**3 m**	**2 m**	**3 m**	**2 m**	**3 m**
1	17.5 %	17.5 %	20 %	12.5 %	45 %	17.5 %
3	20 %	12.5 %	20 %	7.5 %	32.5 %	17.5 %
5	17.5 %	12.5 %	17.5 %	5 %	35 %	10 %
11	17.5 %	10 %	15 %	2.5 %	15 %	7.5 %

Table 2

[0087] In accordance with an embodiment of the present invention, instructions configured to be executed by a processor to perform a method are stored on a

computer-readable medium. The computer-readable medium can be a device that stores digital information. For example, a computer-readable medium includes a compact disc read-only memory (CD-ROM) as is known in the art for storing software. The computer-readable medium is accessed by a processor suitable for executing instructions configured to be executed. The terms "instructions configured to be executed" and "instructions to be executed" are meant to encompass any instructions that are ready to be executed in their present form (e.g., machine code) by a processor, or require further manipulation (e.g., compilation, decryption, or provided with an access code, etc.) to be ready to be executed by a processor.

[0088] As used to describe embodiments of the present invention, the term "coupled" encompasses a direct connection, an indirect connection, or a combination thereof. Two devices that are coupled can engage in direct communications, in indirect communications, or a combination thereof. Moreover, two devices that are coupled need not be in continuous communication, but can be in communication typically, periodically, intermittently, sporadically, occasionally, and so on. Further, the term "communication" is not limited to direct communication, but also includes indirect communication.

[0089] Embodiments of the present invention relate to data communications via one or more networks. The data communications can be carried by one or more communications channels of the one or more networks. A network can include wired communication links (e.g., coaxial cable, copper wires, optical fibers, a combination thereof, and so on), wireless communication links (e.g., satellite communication links, terrestrial wireless communication links, satellite-to-terrestrial communication links, a combination thereof, and so on), or a combination thereof. A communications link can include one or more communications channels, where a communications channel carries communications. For example, a communications link can include multiplexed communications channels, such as time division multiplexing ("TDM") channels, frequency division multiplexing ("FDM") channels, code division multiplexing ("CDM") channels, wave division multiplexing ("WDM") channels, a combination thereof, and so on.

[0090] Systems and methods in accordance with an embodiment of the present invention disclosed herein can advantageously increasing the scalability and decrease the cost of tracking and identifying humans moving within a fixed space.

[0091] The foregoing disclosure of the preferred embodiments of the present invention has been presented for purposes of illustration and description. It is not intended to be exhaustive or to limit the invention to the precise forms disclosed. Many variations and modifications of the embodiments described herein will be apparent to one of ordinary skill in the art in light of the above disclosure. The scope of the invention is to be defined only by the claims appended hereto, and by their equivalents.

[0092] Further, in describing representative embodiments of the present invention, the specification may have presented the method and/or process of the present invention as a particular sequence of steps. However, to the extent that the method or process does not rely on the particular order of steps set forth herein, the method or process should not be limited to the particular sequence of steps described. As one of ordinary skill in the art would appreciate, other sequences of steps may be possible. Therefore, the particular order of the steps set forth in the specification should not be construed as limitations on the claims. In addition, the claims directed to the method and/or process of the present invention should not be limited to the performance of their steps in the order written, and one skilled in the art can readily appreciate that the sequences may be varied and still remain within the spirit and scope of the present invention.

WHAT IS CLAIMED IS:

1. A system for identifying an object from movement of the object, comprising:

a sensor for detecting radiation from the object as the object moves over time; and

a processor coupled to the sensor, for converting the detected radiation to a spectral radiation signature, and for comparing the spectral radiation signature to at least a second spectral radiation signature to identify the object.

2. The system of claim 1 wherein the sensor comprises an infrared detector.

3. The system of claim 2 wherein the infrared detector comprises a pyroelectric detector.

4. The system of claim 3 wherein the pyroelectric detector comprises more than one detector element.

5. The system of claim 1 wherein the object is one of an animal, a vehicle, and a human being.

6. The system of claim 1 wherein the sensor comprises a coded aperture.

7. The system of claim 1 wherein the sensor comprises a lens.

8. The system of claim 1 wherein the sensor comprises a Fresnel lens array.

9. The system of claim 8 wherein the Fresnel lens array comprises a mask, wherein the mask comprises at least one zone of visibility.

10. The system of claim 1 wherein a second sensor is used to determine a location of the object.

11. A system for identifying an object from movement of the object , comprising:

a sensor for detecting radiation from the object as the object moves along a first path over time; and

a processor coupled to the sensor; wherein the processor covertns the detected radiation to a spectral radiation signature; and

wherein the processor is adapted:

to obtain temporal radiation data from a second object moving along a second path using the sensor;

to convert the temporal radiation data from the second object to a second spectral radiation signature;

to apply principal components analysis to the second spectral radiation signature to produce underlying factors and scores for the second spectral radiation signature;

to apply a multiple linear regression to the underlying factors and scores to produce a regression vector and a mean and covariance of clustered data for the second spectral radiation signature;

to obtain an inner product of the regression vector and the spectral radiation signature; and

to compare the inner product to the mean and covariance of clustered data to determine if an identity of the object matches the second object.

12. The system of claim 11 wherein the sensor comprises an infrared detector.

13. The system of claim 12 wherein the infrared detector comprises a pyroelectric detector.

14. The system of claim 13 wherein the pyroelectric detector comprises more than one detector element.

15. The system of claim 11 wherein the object is one of an animal, a vehicle, and a human being.

16. The system of claim 11 wherein the sensor comprises a coded aperture.

17. The system of claim 11 wherein the sensor comprises a lens.

18. The system of claim 11 wherein the sensor comprises a Fresnel lens array.

19. The system of claim 18 wherein the Fresnel lens array comprises a mask, wherein the mask comprises at least one zone of visibility.

20. The system of claim 11 wherein a second sensor is used to determine a location of the object.

21. A method for identifying an object from movement of the object, comprising:

obtaining first temporal radiation data from a first object moving along a first path;

converting the first temporal radiation data from the first object to a first spectral radiation signature;

applying principal components analysis to the first spectral radiation signature to produce underlying factors and scores for the first spectral radiation signature;

applying a multiple linear regression to the underlying factors and scores to produce a regression vector and a mean and covariance of clustered data for the first spectral radiation signature;

obtaining second temporal radiation data from a second object moving along a second path;

converting the second temporal radiation data from the second object to a second spectral radiation signature;

obtaining an inner product of the regression vector and the second spectral radiation signature; and

comparing the inner product to the mean and covariance of clustered data to determine if an identity of the first object matches the second object.

22. The method of claim 21 wherein the first object is one of an animal, a vehicle, and a human being.

23. The method of claim 21 wherein the second object is one of an animal, a vehicle, and a human being.

24. The method of claim 21 wherein obtaining first temporal radiation data and obtaining first temporal radiation data comprise using a sensor to detect radiation from the first object over time and using the sensor to detect radiation from the second object over time.

25. The method of claim 24 wherein the sensor comprises an infrared detector.

26. The method of claim 25 wherein the infrared detector comprises a pyroelectric detector.

27. The method of claim 26 wherein the pyroelectric detector comprises more than one detector element.

28. The method of claim 24 wherein the sensor comprises a coded aperture.

29. The method of claim 24 wherein the sensor comprises a lens.

30. The method of claim 24 wherein the sensor comprises a Fresnel lens array.

31. The method of claim 30 wherein the Fresnel lens array comprises a mask, wherein the mask comprises at least one zone of visibility.

32. A system for identifying a human being from movement of the human being, comprising:

a dual element pyroelectric detector, wherein the dual element pyroelectric detector detects radiation from the human being as the human being moves over time;

a Fresnel lens array, wherein the Fresnel lens array is located between the dual element pyroelectric detector and the human being, wherein the Fresnel lens array comprises a mask, and wherein the mask comprises at least one zone of visibility; and

a processor, wherein the processor is coupled to the dual element pyroelectric detector, the processor converts the detected radiation to a spectral radiation signature, and the processor compares the spectral radiation signature to at least a second spectral radiation signature to identify the human being.

33. A system for identifying a human being from movement of the human being, comprising:

a dual element pyroelectric detector, wherein the dual element pyroelectric detector detects radiation from the human being as the human being moves along a first path over time;

a Fresnel lens array, wherein the Fresnel lens array is located between the dual element pyroelectric detector and the human being, wherein the Fresnel lens array comprises a mask, and wherein the mask comprises at least one zone of visibility; and

a processor; wherein the processor is coupled to the dual element pyroelectric detector; wherein the processor converts the detected radiation to a spectral radiation signature; and

wherein the processor is adapted:

to obtain temporal radiation data from a second human being moving along a second path using the sensor;

to convert the temporal radiation data from the second human being to a second spectral radiation signature;

to apply principal components analysis to the second spectral radiation signature to produce underlying factors and scores for the second spectral radiation signature;

to apply a multiple linear regression to the underlying factors and scores to produce a regression vector and a mean and covariance of clustered data for the second spectral radiation signature;

to obtain an inner product of the regression vector and the spectral radiation signature; and

to compare the inner product to the mean and covariance of clustered data to determine if an identity of the human being matches the second human being.

APPENDIX 1

SUBMITTED TO IEEE TRANSACTIONS ON SYSTEM, MAN, AND CYBERNETICS, PART A

Tracking and Identifying Multiple Humans with Wireless Geometric Pyroelectric Sensors

Qi Hao, Jian-Shuen Fang, David J. Brady, Bob D. Guenther, and Mohan Shankar

Abstract—**This paper presents a description of a wireless pyroelectric sensor system, whose sensing visibilities are modulated by Fresnel lens arrays, for tracking and identifying multiple humans. The concept of a geometric sensor is discussed and utilized in local/global visibility modulation for the node-centric sensor system, to implement the process of data-object-association and walker feature extraction. An Expectation-Maximization-Bayesian tracking scheme, consisting of detection, localization, filtering, and prediction, is proposed and implemented among slave, master, and host modules of a prototype sensor system. Experimentally the prototype system was able to simultaneously track two individuals and recognize five individuals with an average success rate of 86 %.**

Index Terms—**Multiple human tracking, human identification, pyroelectric sensor, Fresnel lens, visibility modulation**

I. Introduction

Multiple human tracking is desirable yet challenging for many applications: surveillance, smart video conference, computer vision, robotics and intelligent space, just to name a few [1], [2], [3], [4], [5]. It tends to be ambiguous and confusing as objects are often occluded by others in the field of view (FOV) of the sensors. From the perspective of trackers, the tracking errors of one object may propagate into those of others. Object identification has been proposed to help reduce such mutual interference in tracking [6], [7]. Besides, the varying number of objects within observation space gives rise to the issue of object number determination [8].

Most trackers consist of four components, namely object representation, localization, data-object-association, and motion filtering [3]. The way to implement all these parts in tracking is application dependent and the various approaches differ in robustness and efficiency. For real-time applications, the system resource for tracking is limited and the computational complexity of a tracker should be minimized. In video based applications, where the nonrigid aspect of objects are of more interest, object feature extraction and representation play an important role and consume most of the computation resources [2], [3], [9]. For acoustic sensor tracking systems, by contrast, objects are assumed rigid and signal-to-noise ratios (SNRs) are low due to the noisy and clutter filled environments. Numerous data-object-association and motion filtering techniques have been proposed and developed, from multiple hypothesis trackers (MHTs) [10], [11] to joint probability data association filters (JPDAFs) [12], [13], [14], sequential Monte Carlo simulations [15], [16], and a variety of Bayesian filtering schemes [17].

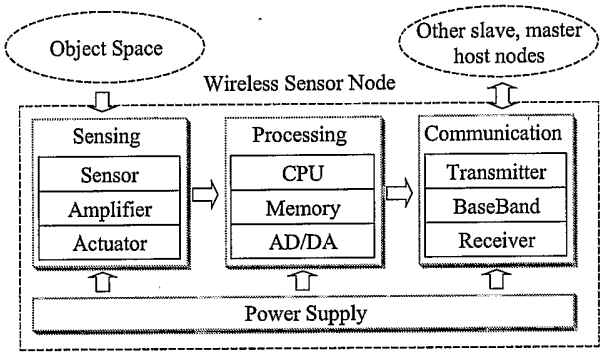

Fig. 1. Sensor node architecture.

Recent advances in micro-processors, radio frequency transceivers, sensors, and networking techniques enable traditional centralized multiple sensor systems to evolve into new generations of *ad hoc*, wireless, distributed sensor networks (DSNs) [18]. In a typical DSN, small, low-cost, spatially dispersed sensor nodes, as illustrated in Fig. 1, with their own computation and communication capabilities, collaborate with each other to achieve complicated tasks [7], [19], [20]. For most DSN applications, passive sensors are preferred to active ones because of their low costs, low power consumption, and low detectability. A low cost passive infrared (PIR) motion detector, the pyroelectric $LiTaO_3$ with its visibility manipulated by a Fresnel lens array [21], [22], [23], [24], [25], [26], [27] is the passive sensor selected for the research described here.

The underlying mechanism of human tracking and identification to be discussed includes multiplex sensing techniques and the concept of geometric sensors [28], [29]. A multiplex sensing technique enables each sensor to take measurements that depend jointly on multiple source points in the object space under examination. The linear combinations of object data can increase the mean power per measurement and thus the signal-to-noise ratio in the presence of additive noise. The multiplex advantage is substantial in the infrared, where thermal noise dominates. The multiplex sensing technique also allows the source motion to be captured. In this work, an 11-element Fresnel lens array produces 11 visibilities for a single pyroelectric sensor. The spectral content of the response

Manuscript created Mar. 18, 2006. This work is supported by Army Research Office through the grant DAAD 19-03-1-03552.

J.-S. Fang is with the Department of Photonics & Institute of Electro-Optical Engineering, National Chiao Tung University, 1001 Ta Hsueh Rd., Hsinchu 300, Taiwan. The rest of the authors are with the Fitzpatric Center for Photonics and Communications, Duke University, Durham NC 27708, USA (email:qh@ee.duke.edu)

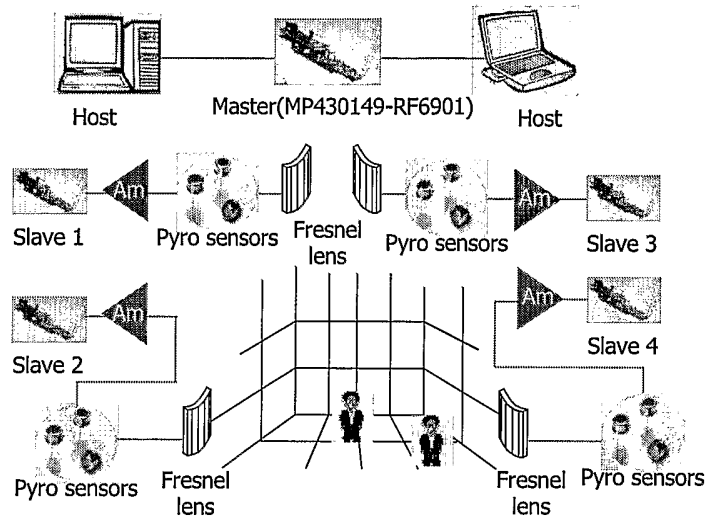

Fig. 2. The setup of the distributed wireless pyroelectric sensor system.

data, as a human walks through the 11 areas, can be used to discriminate between multiple individuals. The spectral signatures are believed to be caused by the difference in the motion of arms and legs [30].

The concept of geometric sensors assumes that the radiation field that propagates from the object space to the measurement space is characterized by a simple ray propagation model rather than a wave propagation one. By manipulating the global and local visibilities of the sensors, the redundant radiation information can be filtered out [31], [32], [33]. For example, a Fresnel lens can shape the visibilities of pyroelectric sensors so that when humans enter different regions, different sets of sensors can fire, generating signal patterns and identifying locations of people. For each sensor, however, a trade-off between global and local visibility modulation has to be made. A large global visibility is more efficient in area coverage but at the expense of increased location ambiguities. Local visibilities can uniquely label regions of space and as an additional benefit generate signals that can be used to identify a person [34].

The ultimate goal of our work is to develop a wireless distributed pyroelectric sensor network, which can track multiple humans in a confined area, while maintaining their identities, as illustrated in Fig. 2. The challenges for tracking multiple humans with distributed pyroelectric sensors include

1) high variability of human motions and their thermal biometrics;
2) decreased range of a pyroelectric sensor when its lens apertures are reduced for modulation;
3) errors in geometric optics modeling and in sensor system alignment;
4) limits imposed by sensor number, local computation capabilities, and communication bandwidth.

The first prototype distributed pyroelectric sensor system was designed with five slave modules, four for tracking and one for identification, one master module, and one host PC. As shown in Fig. 3, the main design issues for building such a distributed pyroelectric sensor system include sensor visibility modulation, embedded computation & communication, and data synthesis. From the computational point of view, the system data can be grouped into different levels.

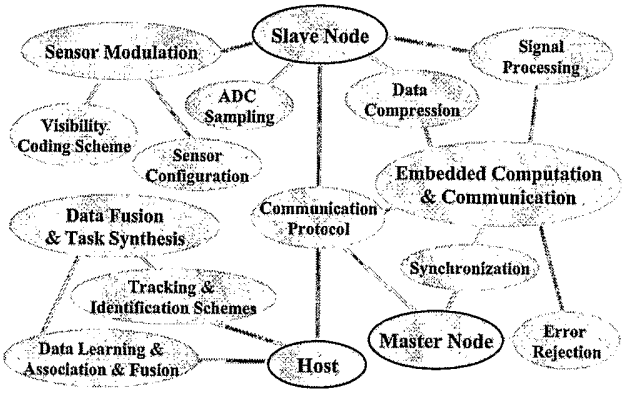

Fig. 3. Main issues for distributed pyroelectric sensor system building.

1) Signal: This is the lowest level of abstraction where sensory data from distributed and clustered slaves are captured, digitalized, and processed locally before broadcasting to a master node;
2) Event: This is a spatial-temporal pattern represented by an 8-bit index. It represents the on/off status of eight sensors of one slave node. It contains information about the angular displacement measurement with respect to this slave node.
3) Feature: This is a pattern made up of 4-bit event indexes. It is associated with registered objects and used to distinguish them from each other.

4) Object: This is the source of a pattern defined in the spatial domain. In our study, an object is a walker whose identity is associated with a feature.
5) Template: This is a pattern of multiple objects, such as the number of people in the object space and their identities.

Each slave module for tracking contains eight pyroelectric sensors with modulated visibilities to measure the angular displacements of thermal sources. The slave module for identification contains four sensors, whose visibilities are modulated with different codes for use in identification. Each slave module is able to collect the sensor response signals, convert them into digital event indexes, by filtering, threshold testing, and smoothing, and send them to the master module via a wireless channel. The master module collects event indexes from the slave modules, and synthesizes those from tracking slaves into one composite event message, while synchronizing the communications and rejecting the event errors. The master module sends the processed messages to the host which converts the event messages into local bearing measurements, into walker features, and into the number of objects present. The host then fuses all the data, through a Bayesian tracking scheme and likelihood comparison, to estimate the motion trajectories and the identities of objects.

In this paper, we present a framework for tracking and identifying multiple humans by using distributed wireless geometric pyroelectric sensors. The multiple human tracking problem includes four parts: detection, to extract events from the sensor data; localization, to decompose event messages into individual parts and associate them with each object; filtering, to smooth the object trajectories by using their motion *prior* and observation likelihood models; and prediction, to estimate the states before the next batch of measurements. The identification problem comprises two phases: data training, to build up statistical models of features, and hypothesis testing, to estimate the association likelihood of a new feature. The whole system is event based. The data of each event is packed in a few bytes and transmitted via wireless channels.

Section II describes the system setup, the sensor model, the sensor modules, and the visibility modulation with masked Fresnel lens arrays. Section III presents a mathematical description of the problems of multiple human tracking and human identification. Section IV investigates the event capture, processing, and analysis for tracking and identification. Section V describes the data association, fusion, tracking synthesis, and hypothesis testing on the host side. Section VI summarizes the system implementation. section VII shows experimental results, and discusses the strength and weakness of the sensor system and its potentials. Section VIII outlines future work.

II. System Model and Sensor Modules

In this section, we present a pyroelectric sensor system model and the technique of visibility modulation with Fresnel lens arrays. The design and development of sensor modules for tracking and identification are also described.

A. Pyroelectric Sensor Modeling

In our study, pyroelectric sensing circuits create the signal space, Fresnel lens arrays produce the visibility modulation, and human thermal sources form the object space.

Under the linearity assumption, the response signal of m sensors, $\mathbf{s}(t) \in \mathcal{R}^m$, is given by

$$\mathbf{s}(t) = h(t) * \int_{\Omega} \mathbf{v}(\mathbf{r})\psi(\mathbf{r},\ t)d\mathbf{r} \qquad (1)$$

where "$*$" denotes convolution, $h(t)$ is the impulse response of one sensor, Ω is the object space, $\mathbf{v}(\mathbf{r}) \in [0,1]^m$ is the modulated visibility function between m sensors and the object space, $\psi(\mathbf{r},\ t)$ is the radiation from the object. More details about the visibility and impulse response of a dual element pyroelectric detector and Fresnel lens array described in [27], [30], [33].

From Eq. (1), it can be seen that the sources distribution $\psi(r)$ is indeed a hidden variable. This is to suggest, a comprehensive tracking strategy, *i.e.* a recursive estimation of $\psi(r,t)$, should be developed in an expectation maximization (EM) scheme [35], [36],

- E step: to estimate $\psi(r)$, after updating $r(t)$;
- M step: to estimate $r(t)$, after updating $\psi(r)$.

B. Sensor Modules with Visibility Modulation

The Fresnel lens we employ is made of a light-weight, low-cost plastic material with good transmission characteristics in the $5\sim14\ \mu m$ range. Fig. 4 shows the beam pattern produced by the Fresnel lens (AA0.9GIT1, Fresnel Technologies). We utilize the Fresnel lens array to modulate the visibility of our sensors, such that each sensor can observe events uniformly distributed over 11 angles.

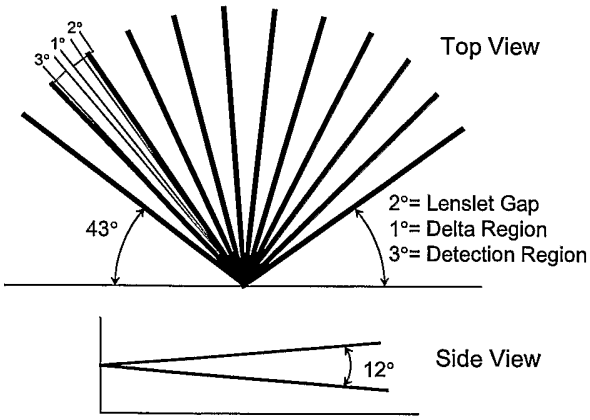

Fig. 4. Top view and side view of the visible zones of a Fresnel lens array when it is placed in front of one pyroelectric sensor. Details of the beam pattern are shown on the second beam from the left.

In the experiments, we made two kinds of sensor modules, one for identification and another for tracking. To generate digital event sequences that contain the distinguishable features of individuals, the FOVs of sensors in each module should be of different visibility modulation over a common region.

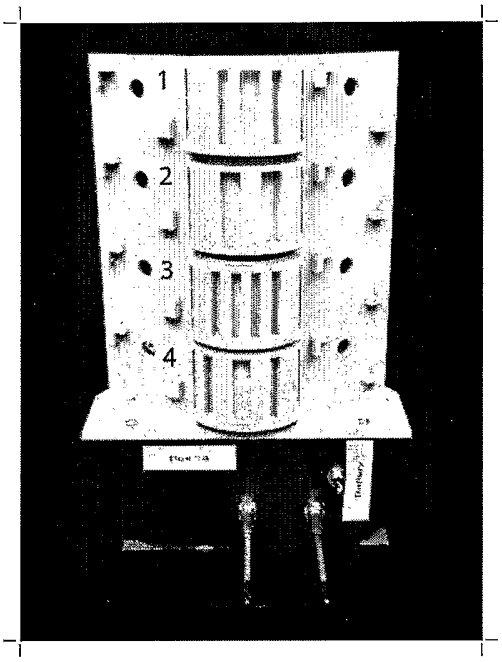

Fig. 5. The single-column radial sensor module for identification.

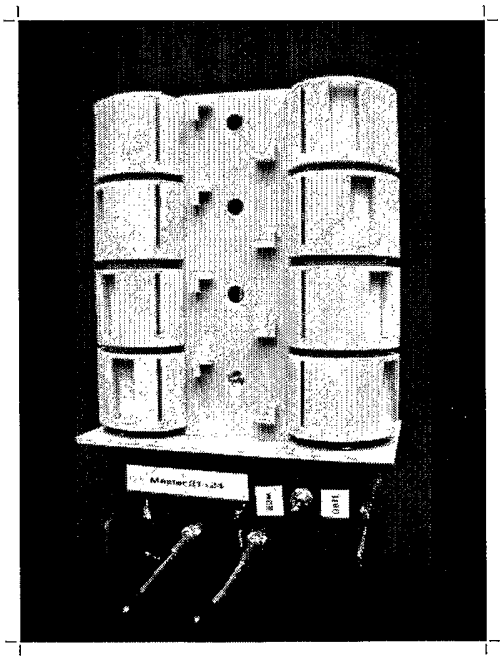

Fig. 6. The two-column radial sensor module for tracking. For each column of sensors, seven detection regions are formed with or without overlapped sensor FOVs.

TABLE I

VISIBILITY CODING SCHEME OF THE IDENTIFICATION NODE

Lens Array	Visibility
1	[0 0 0 1 0 1 1 0 1 0 0]
2	[0 0 0 1 1 0 0 1 1 0 0]
3	[0 0 1 0 1 0 1 0 1 0 0]
4	[0 1 0 0 1 1 0 0 1 0 0]

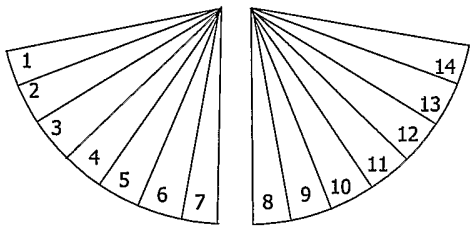

Fig. 7. Visibilities of one tracking sensor module.

To extract digital event index sequences that can track human motion over a large space, the FOVs of sensors in each module should have an identical visibility pattern.

The single column sensor module for identification is shown in Fig. 5. This sensor module has four pyroelectric detectors with aperture modified Fresnel lenses arranged in one column. The FOV of each sensor is modulated according to pseudo-random codes. Table I lists the association between detection regions and the four sensors, shown in Fig. 5.

The two-column radial type of sensor module for tracking is shown in Fig. 6. This sensor module has eight pyroelectric detectors with the Fresnel lens arrays arranged in two columns. In each column, the FOV of each sensor spans 24^0, *i.e.* uses three Fresnel lenses, and there is a 16^0 shift in the FOV between each of four sensors. Two separable detection areas of 72^0 are formed by the two columns. Each detection area comprises seven detection regions with different sensor visibilities, as shown in Fig. 7. The average angular resolution of the sensor module is hence 10^0. Such a visibility design also can facilitate the process of data-object-association: when sensors of one node associated with two different detection areas fire, it can be assumed that there are at least two objects moving. Table II lists the association between detection regions and 8 sensors.

When four of the above tracking nodes are deployed in a $9\ m \times 9\ m$ room, we have a global visibility distribution shown in Fig. 8. It can be seen that four local detection areas are formed in such a deployment, marked as area I, II, III, and IV. In each local area, if only one object moves, those associated sensors can provide high angular resolution. The detection range of each sensor can be reduced to its local areas by increasing the value of firing threshold set in the embedded signal processor. Given such a visibility configuration, the number of human objects to be tracked can be no more than four and the whole data-object-association scheme is accomplished in two steps: identify the local area of

TABLE II
VISIBILITY CODING SCHEME OF THE TRACKING NODE

Detection Region	Sensors
1	[1 0 0 0 0 0 0 0]
2	[1 1 0 0 0 0 0 0]
3	[0 1 0 0 0 0 0 0]
4	[0 1 1 0 0 0 0 0]
5	[0 0 1 0 0 0 0 0]
6	[0 0 1 1 0 0 0 0]
7	[0 0 0 1 0 0 0 0]
8	[0 0 0 0 1 0 0 0]
9	[0 0 0 0 1 1 0 0]
10	[0 0 0 0 0 1 0 0]
11	[0 0 0 0 0 1 1 0]
12	[0 0 0 0 0 0 1 0]
13	[0 0 0 0 0 0 1 1]
14	[0 0 0 0 0 0 0 1]

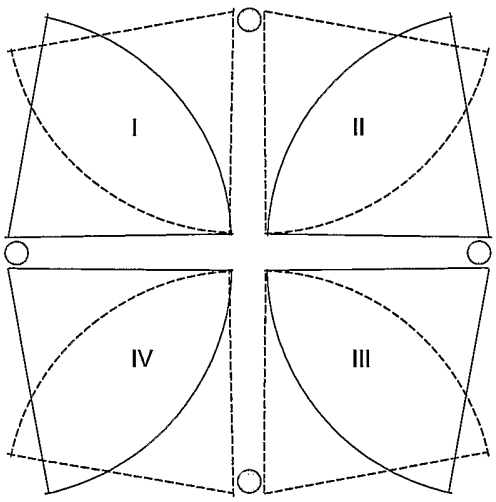

Fig. 8. Visibilities of four sensor modules and four local detection areas formed for event validation to reduce false alarms.

an object and identify the angular displacement measurements associated with this object.

III. Problem Formulation

In this section, we present the multiple human tracking problem in terms of object motion dynamics and a sensor observation model. The walker identification problem can be divided into two steps: data learning and hypothesis testing, based on hidden Markov models.

A. Multiple Human Tracking

In the configuration space, the configuration state $\mathbf{x}(t)$, served to represent spatial-temporal varying radiation from the objects, $\psi(\mathbf{r},\ t)$, for example, their positions and velocities in a 2-D plane. Under the discrete sampling scheme, the l^{th} object state at time k is a random vector $\mathbf{x}_k^l$. The object state evolution can be modeled by the following linear system equation:

$$\mathbf{x}_{k+1}^l = \Phi \mathbf{x}_k^l + \Gamma^l \mathbf{w}_k^l \tag{2}$$

where the object label $l = 1, ..., L$, the object position and displacement $\mathbf{x}_k^l = [x_k^l,\ \delta x_k^l,\ y_k^l,\ \delta y_k^l]^T$, the dynamics uncertainty $\mathbf{w}_k = [w_{xk},\ w_{yk}]^T$,

$$\Phi = \begin{bmatrix} 1 & 1 & 0 & 0 \\ 0 & 1 & 0 & 0 \\ 0 & 0 & 1 & 1 \\ 0 & 0 & 0 & 1 \end{bmatrix},\ \Gamma^l = \begin{bmatrix} \gamma^l & 0 \\ 1 & 0 \\ 0 & \gamma^l \\ 0 & 1 \end{bmatrix}.$$

Here, $0 < \gamma^l < 1$, x and y denote the Cartesian coordinates of the object, δ_x and δ_y denote the displacements between two events in the x and y directions, respectively, roughly proportional to the velocities in the two directions. The system noise is zero mean Gaussian white noise, that is, $\mathbf{w}^l \sim \mathcal{N}(\mathbf{0}, \sigma_{wl}^2 \mathbf{I}_2)$, where $\mathbf{I}_2$ is the 2×2 identity matrix. The initial state $\mathbf{x}_0$ describes the objects' initial positions and displacements. A *prior* for the initial state $p(\mathbf{x}_0^l)$ also needs to be specified for the model; we assume $\mathbf{x}_0^l \sim \mathcal{N}(\mathbf{0}, \mathbf{P}_0^l)$.

The dynamics model in Eq. 2 is Markov and can be represented by the conditional density $p(\mathbf{x}_{k+1}|\mathbf{x}_k)$. The problem can be stated as, how to determine the object configuration state sequence $\mathbf{x}_{1:k} = [\mathbf{x}_1, \cdots, \mathbf{x}_k]$ with maximum posterior probability from sensor response signals $\mathbf{s}_{1:k} = [\mathbf{s}_1, \cdots, \mathbf{s}_k]$, given the observation model likelihood $p(\mathbf{s}_k|\mathbf{x}_k)$ and state dynamics *prior* $p(\mathbf{x}_{k+1}|\mathbf{x}_k)$,

$$\mathbf{x}_{1:k} = \arg\max_{\mathbf{x}} p(\mathbf{x}_{1:k}|\mathbf{s}_{1:k}). \tag{3}$$

Note that $p(\mathbf{s}_k|\mathbf{x}_k)$ is derived from the sensor model, visibility function, and *prior* on noise. It is known as the maximum a *posterior* (MAP) Bayesian tracking problem.

By using the visibility coding scheme in Table II, the sensor response signals $\mathbf{s}_{1:k}$ can be digitized into event indexes and then interpreted as angular displacements with respect to each sensing node $z_{1:k}^{(i,j)}$. To form the new observation likelihood model $p(\mathbf{z}_k|\mathbf{x}_k)$, the measurement equation is written as

$$z_k^{(i,j)} = \begin{cases} tan^{-1}\left[\frac{y_k^l - y^{(i,j)}}{x_k^l - x^{(i,j)}}\right] + v & \text{if event } (i,j) \text{ happens;} \\ 0 & \text{otherwise.} \end{cases} \tag{4}$$

where event (i,j) means a motion detection in the j^{th} detection region of the i^{th} node whose origin is $[x^{(i,j)},\ y^{(i,j)}]$, the measurement noise v is a zero mean Gaussian white noise, that is, $v \sim \mathcal{N}(0, \sigma_v^2)$, measurement z is a random variable uniformly distributed over a set of angles $[\theta_1^{(i,j)}, \cdots, \theta_M^{(i,j)}]$.

To handle the possible occlusion of multiple persons, local visibilities are designed for event validation, shown in Fig. 8. When event indexes from four sensor nodes are received, an area-object-association is made first according to the global sensor visibility geometry shown in Fig. 8 and Fig. 14. After such a measurement validation, only two measurements are associated with one object, denoted as,

$$z_k^{(l)} = \left\{ z_k^{(i,j)} : Pr\left[\chi_k^{(l,i,j)}\right] > 0 \right\}. \tag{5}$$

where $\chi_k^{(l,i,j)}$ is the event that measurement $z_k^{(i,j)}$ originates from the l^{th} object.

The general sequential Bayesian tracking problem requires that we recursively calculate some degree of belief in the state $\mathbf{x}_k^l$ with validated measurements $\mathbf{z}_{1:k}^{(l)}$. Its solution includes two parts: prediction and filtering, given by

$$\begin{aligned} p\left[\mathbf{x}_k^l|\mathbf{z}_{1:k-1}^{(l)}\right] &= \int p\left[\mathbf{x}_k^l|\mathbf{x}_{k-1}^l\right] p\left[\mathbf{x}_{k-1}^l|\mathbf{z}_{1:k-1}^{(l)}\right] d\mathbf{x}_{k-1}^l, \\ p\left[\mathbf{x}_k^l|\mathbf{z}_{1:k}^{(l)}\right] &= \frac{p\left[\mathbf{z}_k^{(l)}|\mathbf{x}_k^l\right] p\left[\mathbf{x}_k^l|\mathbf{z}_{1:k-1}^{(l)}\right]}{p\left[\mathbf{z}_k^{(l)}|\mathbf{z}_{1:k-1}^{(l)}\right]}, \end{aligned} \quad (6)$$

where $p\left[\mathbf{z}_k^{(l)}|\mathbf{z}_{1:k-1}^{(l)}\right]$ can be viewed as a normalizing constant. The probabilistic model of the state evolution $p\left[\mathbf{x}_k^l|\mathbf{x}_{k-1}^l\right]$ is defined by the system equation in Eq. (2) and the known statistics of $\{\mathbf{w}_k\}$. The likelihood function $p\left[\mathbf{z}_k^{(l)}|\mathbf{x}_k^l\right]$ is defined by the measurement equation in Eq. (4) and the known statistics of $\{v_k\}$.

B. Walker Identification

An HMM can be set up as

1) $S = \{s_1, s_2, ..., s_T\}$: hidden state sequence.
2) $X = \{x_1, x_2, ..., x_T\}$: feature sequence.
3) $\mathbf{A} = \{a_{ij}\}$, $a_{ij} = P(s_{t+1} = j|s_t = i)$: state transition probability matrix.
4) $\mathbf{B} = \{b_{im}\}$, $b_{im} = P(x_t = m|s_t = i)$: emission probability matrix.
5) $\pi = \{\pi_i\}$: initial state distribution.
6) $\theta_H = \{\mathbf{A}, \mathbf{B}, \pi\}$: model's parameters.

For a given parameter vector θ_H, the likelihood of the hidden state sequence S and the observed data X to associate with the model is

$$p(X, S|\theta_H) = \left[\prod_{t=1}^{T-1} a_{s_t s_{t+1}}\right]\left[\prod_{t=1}^{T} b_{s_t x_t}\right]\pi_{s_1} \quad (7)$$

To estimate the membership of a feature sequence associated with this model, we estimate the hidden state sequence first and use that to calculate the association likelihood. The *posterior* probability of the hidden states S given X and θ is given by

$$p(S|X, \theta_H) = \frac{1}{\Sigma_S p(X, S|\theta_H)}\left[\prod_{t=1}^{T-1} a_{s_t s_{t+1}}\right]\left[\prod_{t=1}^{T} b_{s_t x_t}\right]\pi_{s_1} \quad (8)$$

The traditional training algorithm for a hidden Markov model is an expectation-maximization (EM) algorithm know as the Baum-Welch algorithm. It is a maximum likelihood method, or, with a simple modification, a penalized maximum likelihood method, which can be viewed as maximizing a posterior probability density over the model parameters. The Baum-Welch algorithm is an iterative algorithm that increase posterior likelihood at each iteration until a maximum is reached. In each iteration, a forward-backward (E) step computes the probabilities of state sequence S conditioned on the current parameters θ, then an M-step updates the parameter θ.

The forward and backward probabilities $\alpha^{(t)}$ and $\beta^{(t)}$ are given by [37]

$$\begin{aligned} \alpha_i^{(1)} &= \pi_i b_{ix_1}, \\ \alpha_j^{(t+1)} &= \left[\Sigma_{i=1}^N \alpha_i^{(t)} a_{ij}\right] b_{jx_{t+1}}, \\ \beta_i^{(T)} &= b_{ix_T}, \\ \beta_i^{(t)} &= b_{ix_t}\left[\Sigma_{i=1}^N a_{ij}\beta_j^{(t+1)}\right]. \end{aligned} \quad (9)$$

The M-step is expressed in terms of $n_{ij}^{(t)}$, the posterior probability that there was a transition between state i and state j at time step t given X and θ,

$$\begin{aligned} n_{ij}^{(t)} &= \Sigma_S P(S|X, \theta)\delta(s_t = i, s_{t+1} = j) \\ &= \frac{1}{Z_n}\alpha_i^{(t)} a_{ij}\beta_j^{(t+1)}, \end{aligned} \quad (10)$$

where Z_n is a normalizing constant such that $\Sigma_{i,j=1}^I n_{ij}^{(t)} = 1$. Then the M-step is [37]

$$\begin{aligned} \pi_i' &= \Sigma_{j=1}^I n_{ij}^{(1)}, \\ a_{ij}' &= \frac{\Sigma_{t=1}^{T-1} n_{ij}^{(t)}}{\Sigma_{t=1}^{T-1}\Sigma_{j'=1}^I n_{ij'}^{(t)}}, \\ b_i' m &= \frac{\Sigma_{t=1}^T \Sigma_{j=1}^I n_{ij}^{(t)}|_{s.t. x_t = m}}{\Sigma_{t=1}^T \Sigma_{j=1}^I n_{ij}^{(t)}}. \end{aligned} \quad (11)$$

For an unlabeled feature, *i.e.* an event sequence, X, we will have $K+1$ hypothesis for K registered objects, $\{H_0, ..., H_K\}$, to test. The hypothesis H_0 represents "none-of-the-above". The decision rule then is

$$X \in \begin{cases} H_0, & \text{if } \max_i\ p(X|H_i) < \gamma \\ H_i : i = arg\ \max_i\ p(X|H_i), & \text{otherwise} \end{cases} \quad (12)$$

where $p(X|H_i)$ is the likelihood of X to associate with the i^{th} hypothesis and γ is the selected acceptance/rejection threshold. There are two special cases: for the verification problem, $i = 1$; for the closed-set identification problem, $\gamma = -\infty$.

IV. Event Generation and Feature Extraction

In general, as shown in Fig. 9, the tracking procedure for distributed sensors includes: event detection, to capture the sensor response signals generated by human motions, digitize them into event indexes, and reject false alarms; object localization, to decompose events into groups and associate different groups of events with different objects based on the prediction of Bayesian tracking and measurement gating; and motion tracking, to estimate the trajectory of objects by Bayesian tracking techniques.

In our implementation, we assign event digitization, including matched filtering, threshold testing, and low-pass filtering, to slave modules. The message between each slave and the master contains a message head and tail plus 2 bytes, the slave ID and the on/off status of the 8 detectors. The master module synchronizes the wireless communication, collects event indexes transmitted from slave modules, and rejects false alarms, *i.e.* a process of event validation.

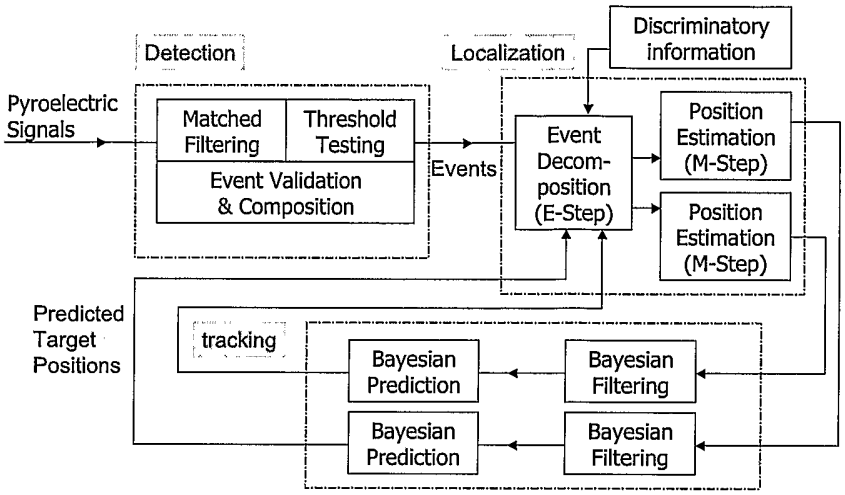

Fig. 9. An EM-Bayesian multiple human tracking scheme for distributed pyroelectric sensors.

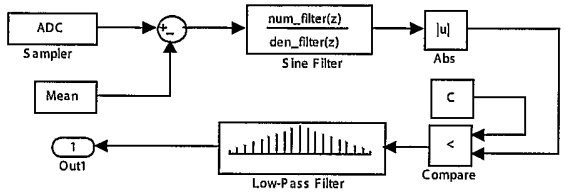

Fig. 10. Block diagram of the filter architecture for event detection.

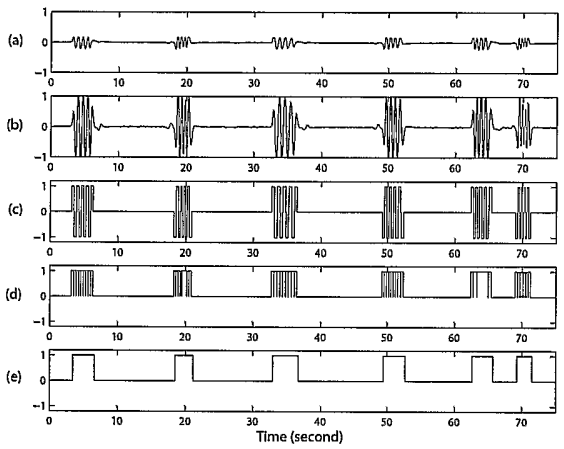

Fig. 11. Event window creation by matched filtering, threshold testing, and low-pass filtering. (a) Raw data. (b) Filtered signals. (c) Digitized signals. (d) Logic signals. (e) Event windows.

A. Event Detection and digitization

From the physical perspective, an event is an occurrence of interest in spatial-temporal space, distinguishable from its environment, and repeatable in multiple trials. In our case, an event is an instance where the thermal flux collected by a pyroelectric sensor is above a preset threshold and where the response data can be associated with specific motion of human objects, such as moving across one detection region.

Fig. 10 shows the embedded signal processing architecture for the event detection. When a human object passes through the Fresnel lens modulated FOV, sine-like response signals are generated. By using a band-pass sine filter, *i.e.* $sin[2\pi(1:N)/N]$, we can capture and amplify the features of interest in the response signals. When a processed signal's absolute value is larger than a threshold, dynamically adjusted according to the noise variance of the sensor, the corresponding bit of the event index is set to '1'; otherwise it is set to '0'. A low-pass (moving average) filter is then used to smooth the event index sequence and create frame event windows. The frame event window is created by the onset and offset event times. Fig. 11 illustrates how the event time windows are generated from the sensory data. Only the binary sensor on/off statuses are transmitted via wireless channels.

B. Tracking Event Analysis

Once we have obtained an 8-bit event index from a sensor module, we can convert it into an angular displacement measurement Fig. 12 illustrates a sequence of events transmitted by one sensor node and its translation into angular displacements.

C. Tracking Event Validation

The master node collects, synchronizes and transmits data. In one cycle, it gathers the events from all the sensor nodes, checks their validity, removes false alarms, and frames a new composite event message sent to the host.

Fig. 13 (a) shows the structure of the data packet transmitted from slaves to the master. The packet contains two bytes of FF as "header", two bytes of 10 as "tail", one byte for node ID, and another byte for event index. In our geometric design,

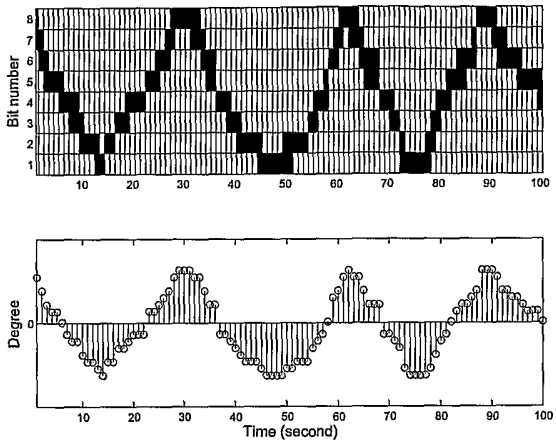

Fig. 12. An 8-bit event sequence from one sensor node and its interpretation as angular displacements.

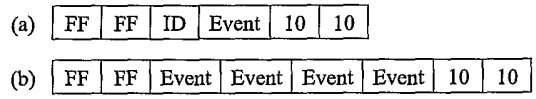

Fig. 13. The structure of event packets, (a) transmitted by slaves via wireless channels, (b) transmitted between the master and the host via a cable.

four local detection areas are formed, shown in Fig. 8. If an object moves inside one of these areas, the sensors associated with that area should fire, forming a valid event. For example, for an object moving in area I of Fig. 14., a legal event has the non-zero four higher bits of the event reported by sensor node 1 and the non-zero four lower bits by sensor node 2. If only one of these two sensors reports a non-zero signal, the master will regard it as invalid and clear those bits to zero. After the event validation, the master will package all four event bytes into a single message, as illustrated in Fig. 13 (b), and send it to the host. The host will localize the objects by interpreting this composite event in an expectation-maximization (EM) way.

D. Feature extraction

The event sequence can also be used for human object identification. From the thermal perspective, each person acts as a distributed infrared source; by properly sampling the IR field, the idiosyncrasies in how an individual carries himself/herself and the habits of how he/she moves, can generate a statistically unique signature. Fig. 15 summarizes the procedure for digital feature extraction. The length of each digital feature is fixed. Once a feature reaches the preset length, the algorithm resets itself awaiting the next batch of event indexes. The sensory data are processed by the embedded micro-controller, and the results are transmitted to the host computer via a wireless channel. Fig. 16 illustrates a down-sampled event index sequences transmitted by the sensor node for identification.

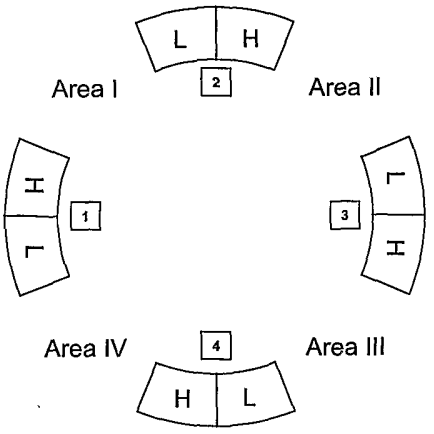

Fig. 14. Event validation made by the master node according to global sensor visibility geometry.

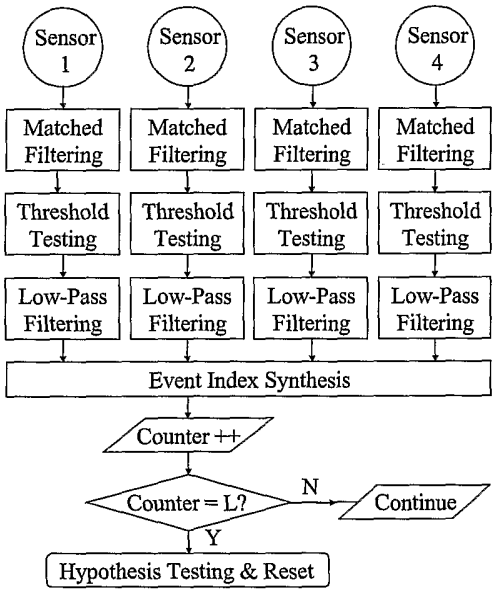

Fig. 15. Digital feature extraction.

V. EM Object Localization

The object localization in most bearing sensor systems is resolved in terms of least square solutions of a set of linear equations. It relies on the *prior* of a sensor observation statistical model only, without taking object motion dynamics into account. The sources are localized to fit the measurements in the maximum likelihood within the Cramér-Rao estimation bound. A grid-approximation can offer a computationally simpler way to translate the angular displacement measurements into Cartesian coordinates.

The more challenging aspect of the multiple object tracking with multiple sensors is the data-object-association problem. It becomes more intractable for sensing systems which only re-

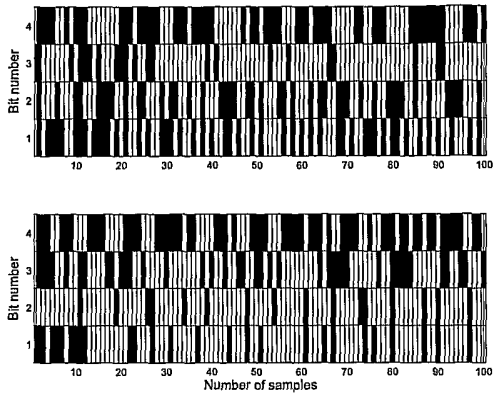

Fig. 16. Two 4-bit event sequences generated by two objects walking along the same path. (a) Bob. (b) Jason.

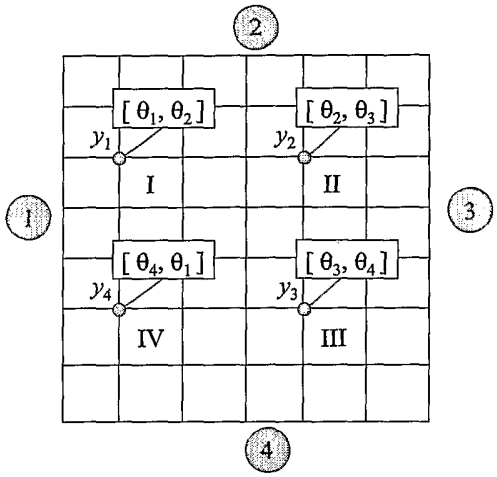

Fig. 17. Grid approximation to linearize the measurements of angular displacements with respect to four sensor nodes.

spond to object motions, because the number of objects varies. We describe an EM scheme for multiple object localization. In each E step, we assume numbers of objects. In each M step, we associate measurements for the assumed number of objects, according to the their last predicted positions and velocities. In other words, we maintain several tracking templates, each of them describing a different number of objects. Over a period, we evaluate all the templates and pick the one with the maximum likelihood for rendering.

A. E Step: Event Decomposition

The composite event received by the host contains the status of all the sensors. Based upon the geometry of the sensor visibilities, the on/off status of the sensors of one tracking slave can be interpreted as an angular displacement in one of its two detection areas. The whole object space is divided into four areas, each of which is associated with sensors of two neighboring slave nodes. After we obtain two angular displacements associated with one object, we convert the bearing measurements to a Cartesain position measurement, $\mathbf{y}_k$, using a grid approximation, shown in Fig. 17.

B. M Step: Measurement-to-Object Association

Three approaches have been studied for reliable and effective data association: multi-hypothesis filtering (MHF), joint probabilistic data association (JPDA), and probabilistic multi-hypothesis filtering (PMHF). The underlying assumption of these probabilistic schemes is that the state is normally distributed according to the latest estimate and covariance matrix, and only the the measurements falling inside validation gates are used. A validation gate is defined as a probability threshold upon the observation likelihood model.

The key concepts of measurement-to-object association for a number of targets are the joint event and and the validation matrix [13]. The joint event is denoted as

$$\chi = \bigcap_{j=1}^{m_k} \chi^{jl_j}, \tag{13}$$

where χ^{jl_j} is the event that the measurement j originated from object l_j, $0 \le l_j \le L$, and l_j is the index of the object to which measurement j is associated, and m_k is the number of validated measurements at time k.

The validation matrix for an join event χ is defined

$$\Omega(\chi) = [\omega_{jl}(\chi)], \tag{14}$$

with ω_{jl} indicating if measurement j lies in the validation gate for object l.

$$\omega_{jl}(\chi) = \begin{cases} 1 & \text{if } \chi^{jl} \text{ occurs} \\ 0 & \text{otherwise.} \end{cases} \tag{15}$$

The construction of each $\Omega(\chi)$ follows the rules [13]:

1) There can be only one origin for a measurement.
2) At most one measurement could have originated from an object.

Those rules might lead to several feasible joint event and validation matrices. To reduce the number of feasible joint events, an individual validation gate can be assumed for each tracker. Only those measurements falling inside the gates will be counted. Fig. 18 illustrates a typical set of validation gates and validation matrices, where $\hat{y}_1$ and $\hat{y}_2$ are estimated object positions, y_1, y_2, and y_3 are position measurements falling insides validation gates, y_4 a position measurement outside gates.

By using Bayes' rule, the probability of one joint event conditioned on all the measurements up to the present time k is obtained as [14],

$$P\{\chi_k|\mathbf{y}_{1:k}\} \propto p[\mathbf{y}_k|\chi_k, \mathbf{y}_{1:k-1}]P\{\chi_k|\mathbf{y}_{1:k-1}\} \tag{16}$$

where $p[\mathbf{y}_k|\chi_k, \mathbf{y}_{1:k-1}]$ is the likelihood of the predicted measurements $\mathbf{y}_k$ for the joint event χ_k, derived from object dynamics and the sensor observation model, and $P\{\chi_k|\mathbf{y}_{1:k-1}\}$ is the *prior* probability of the joint event, derived from the probability distributions of false measurements and of target detection rates [13].

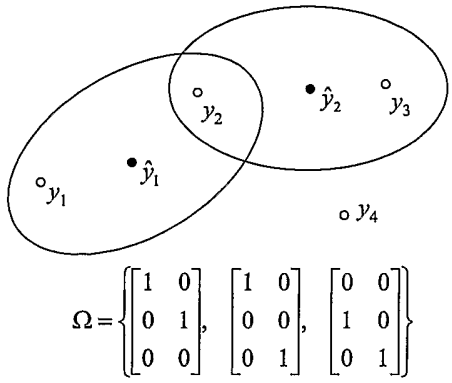

Fig. 18. Typical validation gates and validation matrices.

The association probability β_k^{jl} that measurement j belongs to object l at time k may be obtained by summing over all feasible events for which this condition is true

$$\beta_k^{jl} = \sum_{\chi_k} P\{\chi_k | \mathbf{y}_{1:k}\} \omega_{jl}(\chi_k). \quad (17)$$

The states of each object can be updated with the measurements weighted by those association probabilities.

VI. Data Fusion and Task Synthesis

Multi-sensor data fusion is a process through which we combine measurements from different sensor nodes, remove inconsistencies, and pull all the information together into a coherent structure. Various data fusion schemes and techniques have been proposed for combining measurements from many sensing nodes. Fig. 19 shows the architecture used in our prototype sensor system. Slave nodes work at the raw data level. The master works at the event level. The host carries out the data association and fusion at the object and template level for the purposes of tracking and identification.

A. Template Operation

Our processing scheme is template based. Each template represents a pattern of multiple objects, for example, number of people and their registration status. A template is initialized and terminated based on preselected conditions to save the computation resource. As an example, if after a preselected time only two objects are detected, the templates for four or more objects will be terminated; After some period, the template with the highest likelihood will remain. Similarly for identification, each template contains statistical feature models for one or several enrolled objects. The template with the best fit will report the ID(s) of the recognized object(s).

B. Walker Identification

Walker identification has two parts: data training and hypothesis testing. In the training phase, we use the collected features of individuals to derive HMM feature models. In the testing phase, the log-likelihood of each new feature is

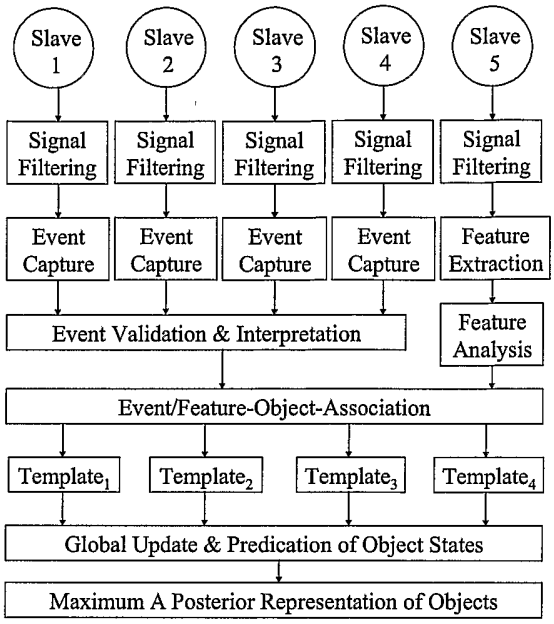

Fig. 19. Data fusion architecture.

evaluated against different walker models. Once a decision is made, an associated pre-recorded 16-bit voice file is played to announce the recognition result.

Hidden Markov models can characterize the statistics of a finite-state sequence for training. Their model parameters θ_H are obtained by random initialization and updated after iterations. By using the MATLAB Statistics Toolbox function *hmmtrain*, we can estimate the transition and emission matrices, **A** and **B**, from an initial guess of their values. With another MATLAB function *hmmdecode*, we can compute the *posterior* state probabilities of testing sequences generated by different walkers. More details about real-time walker recognition using HMMs can be found in [34].

C. Bayesian Filtering and Prediction

After data-object-association processing, the multiple object tracking becomes a set of independent single-object tracking problems. The single-object tracking problem is usually posed as a dynamic estimation of a partially observable Markov process, and in most cases can be solved by Bayesian recursive filtering schemes in the general form of Eq. (6). For the linear and Gaussian tracking problem, Kalman tracking offers the optimal solution. HMM tracking provides the optimal recursion of the *posterior* density estimation, if the state space only consists of a finite number of discrete states. In many situations, linear, Gaussian, or finite discrete state assumptions do not hold. Gaussian approximation, grid-based approximation, and particle filters have been proposed to achieve suboptimal solutions [38].

If the true density is heavily skewed, the Gaussian approximations will have poor performance. Disadvantages of grid-based approach are that its state space must be predefined,

TABLE III

COMPARISON OF DISP ELECTRONIC PLATFORM WITH MOTE

	Duke DISP MSP430149+RF6901 (TI)	Berkeley Mote Atmega128L+NA (Atmel)
MIPS	8	4
Data Width (bits)	16	8
Flash Memory (K)	60	128
Power (active)	0.28mA/M + 32/18mA	2mA/M + 27/10mA
(standby)	1.6μA + 0.6μA	15μA + 1μA
ADC	12bits/8Ch/2.5V/300Ks	10bits/8ch/3.0V/NA
RF Data Rate	76	50
TX power (dBm)	9	5
RX sensitivity(dBm)	-99	-98
OS	NA	TinyOS

which consumes much data storage space, and that each grid point is usually given the same weight, without making good use of object dynamics *prior*. The particle filter technique has heavy computation needs. For real-time implementation, the computation simplicity of a tracking algorithm is more valued than its mathematical rigor.

We summarize the three Bayesian tracking strategies, Kalman, HMM, and Gaussian particle filters, and a comparison of their performances and computation costs is made in [33], [39]. The Kalman tracking scheme based on a grid approximation achieved robust performance with low computation cost and therefore was chosen for our real-time implementation.

VII. SYSTEM IMPLEMENTATION

The complete system consists of slave nodes, containing pyroelectric sensors with Fresnel lens arrays, a master node, and a host computer. We use TRF6901 and MSP430149 as the computation and communication platform. Table III shows the feature comparison between our computation/communication platform [40] and the well-known MOTE processor/radio module [41]. Each slave node also employs an amplifier board in the frequency band $1\sim10$ Hz. More details about our platform can be found in [27], [33].

The distribution of computation load is shown in Fig. 20. Each slave node samples the sensor response signals and converts them into event indexes by band-pass filtering, threshold testing, and low-pass filtering. After compressing each event index into a single byte, the slave node broadcasts the data packet to the master node. The master node synchronizes the communications of the nodes, removes the false alarms, and frames a new composite event message. The master sends the event message to the host, which computes local angular displacements or digital features and updates the dynamics states or identities of objects.

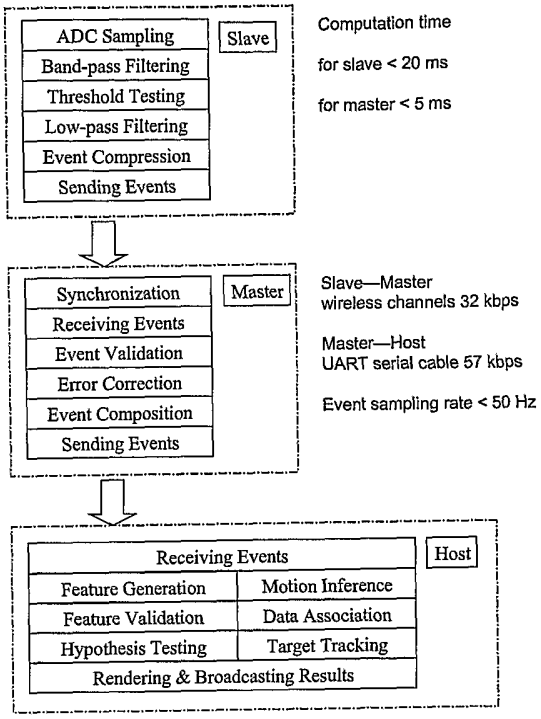

Fig. 20. Computation load distribution among slave, master, and host.

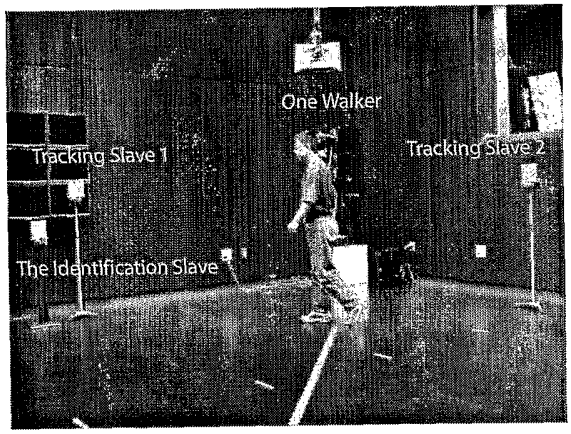

Fig. 21. Photograph of the experiment setup with a single walker.

VIII. RESULTS AND DISCUSSION

The tracking system has been implemented in a 9 $m \times 9$ m room, shown in Fig. 21. First, we tracked one human object walking along a prescribed rectangular path. Then, two human objects were tracked following both the same path and crossing paths. The results of walker identification for arbitrary paths are also given.

A. Case I: One object Tracking

Fig. 22 displays a snapshot of human tracking for one individual with four sensing nodes. The light and dark shaded polygons represent respectively the grid approximation and Kalman estimation of the object position. Each sensor node's angular resolution is roughly $\pi/22$. The four sensing nodes generated 8-bit event sequences shown in Fig. 23. The event sequences were translated into angular displacements and after validation, paired angular measurements were linearized using a grid approximation. The target positions and velocities were estimated and predicted by a Kalman filter. The tracked trajectory of the human object following a prescribed rectangular route is illustrated in Fig. 24. The starting position of the tracker is set as [0 0]. The tracking errors and the histogram of errors are given in Fig. 25. The standard deviation of the

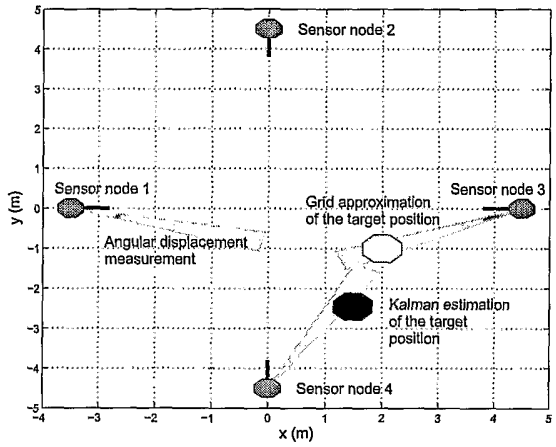

Fig. 22. A snapshot of the one object tracking. Four sensor nodes detect the angular displacements of the target, illustrated as the shaded beams. At each iteration, the target position is estimated by a grid approximation and by Kalman filtering.

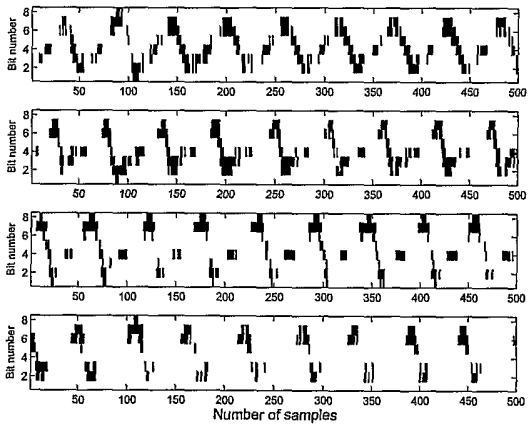

Fig. 23. The 8-bit event sequences of four nodes for one object tracking.

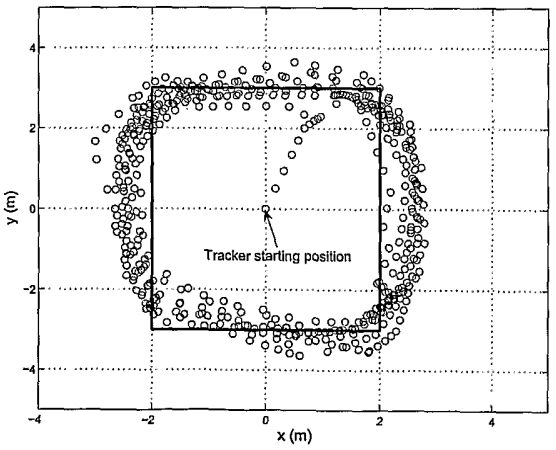

Fig. 24. The estimated trajectory of the human object walking in five rounds. The tracking results are represented by circles and the prescribed route by solid lines.

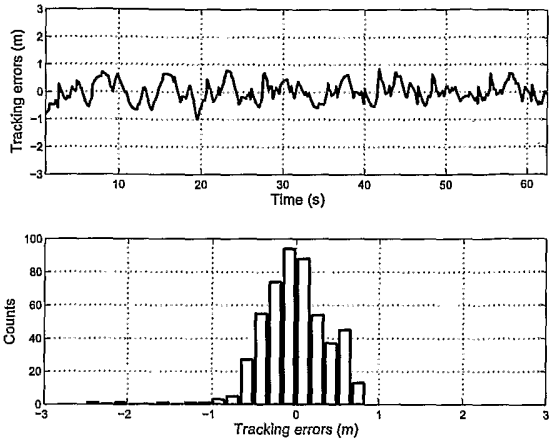

Fig. 25. The tracking errors and their histogram.

tracking errors is 0.4 m.

B. Case II: Two object Tracking

Using the same sensor configuration and algorithm parameters, we tested the tracking performance for two human objects. Fig. 26 displays a snapshot of the tracking of two human objects with four sensing nodes, using the same notation as in Fig. 22. The four sensing nodes generated 8-bit event sequences shown in Fig. 27. Two object tracking involves the process of data-object-association. At each iteration, the association probabilities between measurements and objects were calculated according to Eq. 17 and measurements were assigned to objects accordingly. The tracked trajectories of two human objects following each other along a prescribed rectangular route are illustrated in Fig. 28. It can be seen that both initial positions are set as [0 0]. The tracking errors and their histograms are given in Fig. 29. The standard deviations of the tracking errors are 0.44 m and 0.45 m for the two objects.

A more challenging scenario for multiple object tracking is the case when they walk along different paths with a cross-over. There are indeed no effective solutions for the data association problem in general cases without discrimination characteristics available. For some specific cases, such as when objects don't change their velocities abruptly before and after the cross, we can resolve the data-object-association problem by using the *prior* on speeds and their predictions from Bayesian rules. The four sensing nodes generated 8-bit event sequences shown in Fig. 30. Fig. 31 displays the tracking results when two objects walk along two different diagonals of the room. By using the predicted speeds, the trackers can follow the targets after the cross-over. The tracking errors and their histogram are given in Fig. 32. The standard deviations of the tracking errors are 0.38 m and 0.7 m for Bob and Jason respectively.

C. Case III: Walker Identification

Using HMMs we can identify the walkers following unspecified paths. Each person walks randomly inside a room

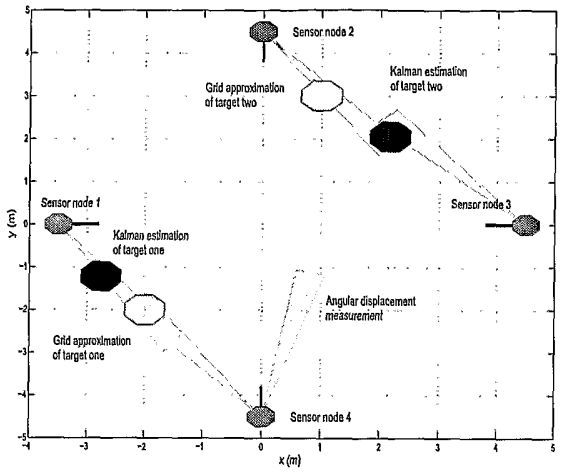

Fig. 26. A snapshot of the two object tracking. Four sensor nodes detect the angular displacements of the target, illustrated as the shaded beams. At each iteration, after the data-object-association, the target positions are estimated by a grid approximation and by Kalman filtering.

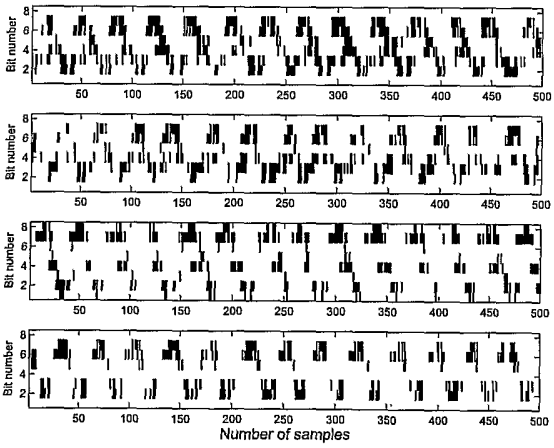

Fig. 27. The 8-bit event sequences of four nodes for two object tracking.

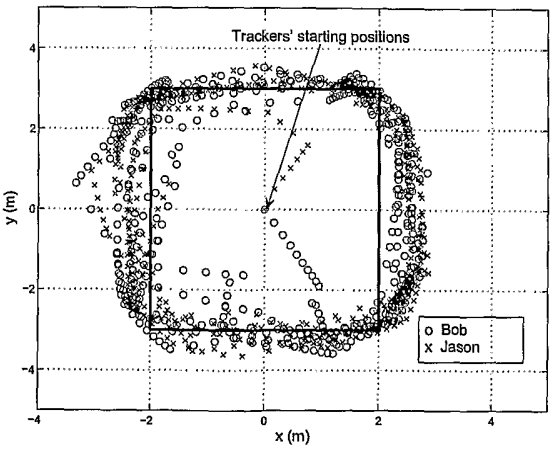

Fig. 28. The estimated parallel trajectories of two human objects walking in five rounds. The tracking results are represented by circles and crosses and the prescribed route by solid lines.

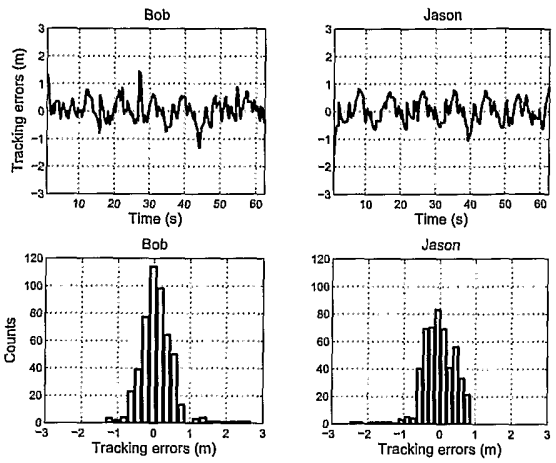

Fig. 29. The tracking errors for two object following parallel paths and the histogram of the entire tracking process is also shown.

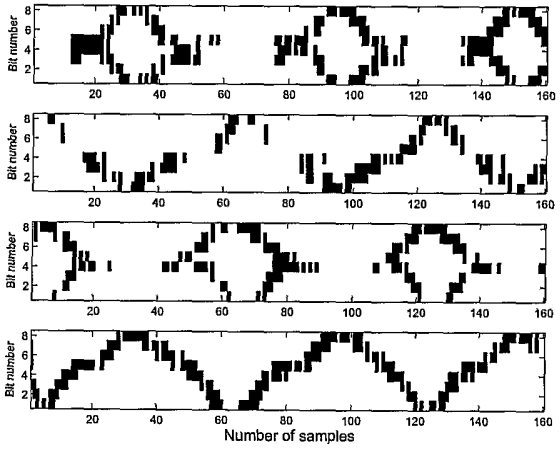

Fig. 30. The 8-bit event sequences of four nodes for tracking two objects having crossing paths.

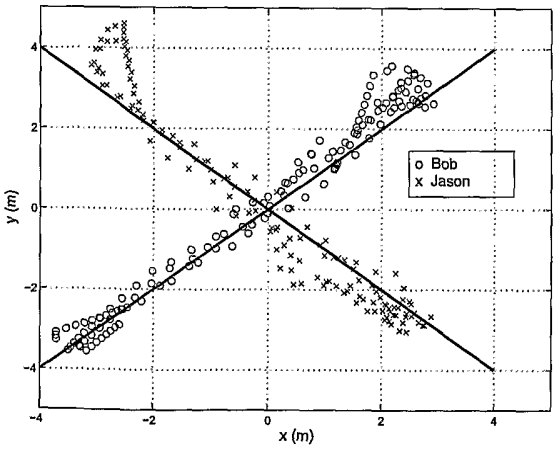

Fig. 31. The estimated crossing trajectories of two human objects walking in three rounds. The tracking results are represented by circles and crosses and the prescribed crossing route by solid lines.

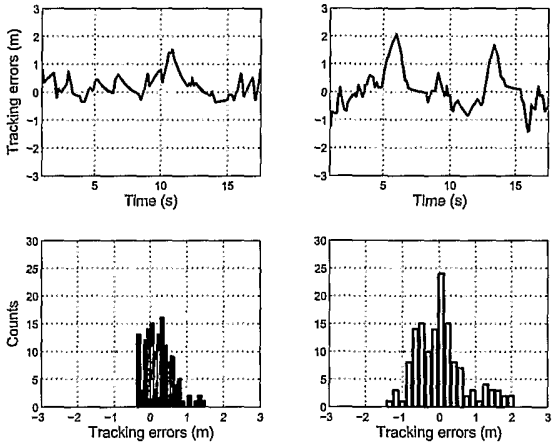

Fig. 32. The tracking errors of two trackers and their histograms.

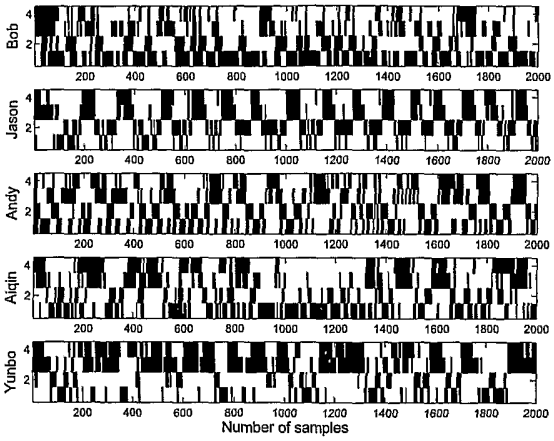

Fig. 33. The 4-bit training sequences of five people who randomly walk inside the room.

for both training and testing. During the training phase, a training event sequence of length 2000 was collected and used to derived an HMM for each person. Fig. 33 shows the training event sequences of five people. During the testing phase, event sequences of length 500 were collected. Each person was tested 20 times. The results of a close-set, path-independent, walker identification of five people are shown in Tab. IV. It can be seen that the lowest successful identification rate is 65%, the highest is 100%, and the average is 86%. More details and more results about walker verification/identification for path-dependent and path-independent scenarios can be found in [34].

D. Discussion

The explicit advantages of human tracking with DSNs include better spatial coverage, robustness, survivability, and modularity. The concept of distributing the computation to multiple low complexity nodes reduce computational requirements of the central processor and the size of data storage. The use of the motion detectors helps maintain the low

TABLE IV

CLOSE-SET PATH-INDEPENDENT IDENTIFICATION RESULTS USING HMMS

Results	Bob	Jason	Andrew	Aiqin	Yunbo
Bob	100%				
Jason		100%			
Andrew			80%	20%	
Aiqin	35%			65%	
Yunbo				15%	85%

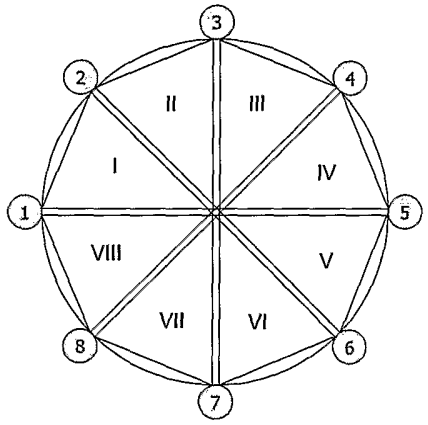

Fig. 34. A general case of sensor deployment for multiple object tracking.

requirements on data throughput, computational consumption, and communication bandwidth. The characteristics of the pyroelectric sensor gives the system the ability to operate under all illumination conditions and the capability to capture human thermal biometrics.

The flexibility and leverage of our geometric sensor paradigm lies in the modular nature of multiplex visibility. It allows improvement in sensing accuracy, tracking precision and signal discrimination among humans and facilitates the process of data-object-association. The trade-off between global and local visibility modulation turns out to be the crucial step in the development of a multiple object tracking system with pyroelectric sensors.

The prototype tracking system presented above only employs four sensor nodes to demonstrate the advantages of geometric sensors in tracking multiple objects. It of course can be extended to more nodes with similar visibility patterns, to achieve higher tracking resolution and capability of tracking more human objects inside a room. A more general case of sensor deployment is illustrated in Fig. 34.

A fully functional real-time multiple human tracking and identification system demands short testing event sequences for fast walker identification and the simultaneous recognition of multiple objects. The identification slave node we used in experiments contains only four pyroelectric sensors. The possible solutions include increasing the number of sensors in the identification node, optimization of the visibility coding, and using multiple identification slave nodes. Other methods such as separating the visibilities of different identification

nodes and choosing the K highest likelihood feature models for a testing event sequence generated by K walkers are also under study.

The motivation of developing geometric sensors in tracking and identification is the study of reference structure tomography [29], which suggests that multi-dimensional features of a radiation source could be captured at an arbitrary level, once there exist such a set of base functions that structurally pose and numerically condition the reconstruction procedure. Through its scan-free multi-dimensional imaging, the feature abstraction, shape parameterization, and even characteristic classification of radiation sources under examination can be achieved in a data-efficient and computation-efficient way. A general visibility design procedure has yet to be proposed, but many visibility coding schemes already have been applied in different coded-aperture imaging systems, from Hadamard codes to pseudo-random codes. [42], [43].

IX. Conclusion

In this paper, we present an implementation of a wireless distributed pyroelectric sensor system for human tracking based on TI's micro-controller and RF transceiver combination of MSP430149 and TRF6901. The system consists of one host, one master, four slave tracking slave, and one identification slave modules. The tracking scheme comprises event detection, object localization, and motion filtering & prediction. The identification node employs specific visibility modulation to identify registered walkers, based on generated event sequences in a fixed length and pre-trained HMMs. The prototype system can track two humans simultaneously in two typical scenarios and identify five walkers with an average success rate of 86%. From the achieved experimental results, we believe that the pyroelectric sensor will rise to one mainstream human detection instrument, besides its video and audio counterparts, and offer one more rich dimension for all the applications of human-machine interfaces. Our future work includes visibility coding optimization, the simultaneous identification of multiple walkers using multiple identification slaves, and an effective integration of multiple human tracking and identification.

References

[1] M. M. Trivedi, K. S. Huang, and I. Mikic, "Dynamic context capture and distributed video arrays for intelligent spaces," *IEEE Trans. Syst., Man, Cybern. A*, vol. 35, no. 1, pp. 145–163, Jan. 2005.

[2] T. Zhao and R. Nevatia, "Tracking multiple humans in complex situations," *IEEE Trans. Pattern Anal. Machine Intell.*, vol. 26, no. 9, pp. 1208–1221, Sept. 2004.

[3] D. Comaniciu, V. Ramesh, and P. Meer, "Kernel-based object tracking," *IEEE Trans. Pattern Anal. Machine Intell.*, vol. 25, no. 5, pp. 564–577, May 2003.

[4] Y. Ricquebourg and P. Bouthemy, "Real-time tracking of moving persons by exploiting spatio-temporal image slices," *IEEE Trans. Pattern Anal. Machine Intell.*, vol. 22, no. 8, pp. 797–808, Aug. 2000.

[5] W. Hu, T. Tan, L. Wang, and S. Maybank, "A survey on visual surveillance of object motion and behaviors," *IEEE Trans. Syst., Man, Cybern. C*, vol. 34, no. 3, pp. 334–352, Aug. 2004.

[6] B. Lin and R. Chellappa, "A generic approach to simultaneous tracking and verification in video," *IEEE Trans. Image Processing*, vol. 11, no. 5, pp. 530–544, May 2002.

[7] D. Li, K. D. Wong, Y. H. Hu, and A. M. Sayeed, "Detection, classification, and tracking of targets," *IEEE Signal Processing Mag.*, vol. 19, no. 2, pp. 17–29, Mar. 2002.

[8] J. Vermaak, S. Maskell, and M. Briers, "Tracking a variable number of targets using the existence joint probabilistic data association filter," *IEEE Trans. Signal Processing*, vol. 33, no. 1, pp. 752–769, Jan. 2005.

[9] C. Stiller and J. Konrad, "Estimating motion in image sequences," *IEEE Signal Processing Mag.*, vol. 16, no. 4, pp. 70–91, July 1999.

[10] R. H. Anderson and J. L. Krolik, "Track association for over-the-horizon radar with a statistical ionospheric model," *IEEE Trans. Signal Processing*, vol. 50, no. 11, pp. 2632–2643, Nov. 2002.

[11] S. S. Blackman, "Multiple hypothesis tracking for multiple target tracking," *IEEE Aerosp. Electron. Syst. Mag*, vol. 19, no. 1, pp. 5–18, Jan. 2004.

[12] Y. Bar-Shalom and T. E. Fortmann, *Tracking and data association*. Reading, CA: Academic Press, 1988.

[13] T. E. Fortmann, Y. Bar-Shalom, and M. Scheffe, "Sonar tracking of multiple targets using joint probabilistic data association," *IEEE J. Oceanic Eng.*, vol. 8, no. 3, pp. 173–184, July 1983.

[14] K.-C. Chang, C.-Y. Chong, and Y. Bar-Shalom, "Joint probabilistic data association in distributed sensor networks," *IEEE Trans. Automat. Contr.*, vol. 31, no. 10, pp. 889–897, Oct. 1986.

[15] C. Hue, J.-P. L. Cadre, and P. Perez, "Sequential monte carlo methods for multiple target tracking and data fusion," *IEEE Trans. Signal Processing*, vol. 50, no. 2, pp. 309–325, Feb. 2002.

[16] T. Vercauteren, D. Guo, and X. Wang, "Joint multiple target tracking and classification in collaborative sensor networks," *IEEE J. Select. Areas Commun.*, vol. 23, no. 4, pp. 714–723, Apr. 2005.

[17] M. Orton and W. Fitzgerald, "A bayesian approach to tracking multiple targets using sensor arrays and particle filters," *IEEE Trans. Signal Processing*, vol. 50, no. 2, pp. 216–223, Feb. 2002.

[18] C.-Y. Chong and S. P. Kumar, "Sensor networks: evolution, opportunities, and challenges," *Proc. IEEE*, vol. 91, no. 8, pp. 1247–1256, Aug. 2003.

[19] J. C. Chen, K. Yao, and R. E. Hudson, "Source localization and beamforming," *IEEE Signal Processing Mag.*, vol. 19, no. 2, pp. 30–39, Mar. 2002.

[20] F. Zhao, J. Shin, and J. Reich, "Information-driven dynamic sensor collaboration," *IEEE Signal Processing Mag.*, vol. 19, no. 2, pp. 61–72, Mar. 2002.

[21] S. B. Lang, "Pyroelectricity: from ancient curiosity to modern imaging tool," *Physics Today*, vol. 58, no. 8, pp. 31–35, Aug. 2005.

[22] S. J. Kang, V. B. Samoilov, and Y. S. Yoon, "Low-frequency response of pyroelectric sensors," *IEEE Trans. Ultrason., Ferroelect., Freq. Contr.*, vol. 45, no. 5, pp. 1255–1260, Sept. 1998.

[23] A. Hossain and M. H. Rashid, "Pyroelectric detectors and their applications," *IEEE Trans. Ind. Applicat.*, vol. 27, no. 5, pp. 824–829, Sept. 1991.

[24] A. Sixsmith, N. Johnson, and R. Whatmore, "Pyroelectric ir sensor array for fall detection in the older population," *J. Phys. IV France*, vol. 128, pp. 153–160, 2005.

[25] A. S. Sekmen, M. Wilkes, and K. Kawamura, "An application of passive human-robot interaction: human tracking based on attention distraction," *IEEE Trans. Syst., Man, Cybern. A*, vol. 32, no. 2, pp. 248–259, Mar. 2002.

[26] T. M. Hussain, A. M. Baig, T. N. Saddawi, and S. A. Ahmed, "Infrared pyroelectric sensor for detection of vehicular traffic using digital signal processing techniques," *IEEE Trans. Veh. Technol.*, vol. 44, no. 3, pp. 683–689, Aug. 1995.

[27] M. Shankar, , J. Burchett, Q. Hao, B. D. Guenther, and D. J. Brady, "Characterization of pyroelectric infrared detectors for human tracking," *Opt. Engr.*, to appear.

[28] D. J. Brady, "Multiplex sensors and the constant radiance theorem," *Opt. lett.*, vol. 27, no. 1, pp. 16–18, Jan. 2002.

[29] D. J. Brady, N. P. Pitsianis, and X. Sun, "Reference structure tomography," *J. Opt. Soc. Am. A*, vol. 21, no. 7, pp. 16–18, July 2004.

[30] J.-S. Fang, Q. Hao, D. J. Brady, B. D. Guenther, J. Burchett, M. Shankar, N. Pitsianis, and K. Y. Hsu, "Path-dependent human identification using a pyroelectric infrared sensor and fresnel lens arrays," *Opt. Exp.*, vol. 14, no. 2, Jan. 2006.

[31] U. Gopinathan, D. J. Brady, and N. P. Pitianis, "Coded aperture for efficient pyroelectric motion tracking," *Opt. Exp.*, vol. 11, no. 18, pp. 2142–2152, Nov. 2003.

[32] Y. Zheng, D. J. Brady, M. E. Sullivan, and B. D. Guenther, "Fiber-optic localization by geometric space coding with a two-dimensional gray code," *Appl. Opt.*, vol. 44, no. 20, pp. 4306–4314, July 2005.

[33] Q. Hao, D. J. Brady, B. D. Guenther, J. Burchett, M. Shankar, and S. Feller, "Human tracking with wireless distributed radial pyroelectric sensors," *IEEE Sensors J.*, submitted for publication.

[34] Q. Hao, J.-S. Fang, D. J. Brady, and B. D. Guenther, "Real-time walker recognition using pyroelectric sensors," *IEEE Trans. Pattern Anal. Machine Intell.*, submitted for publication.
[35] L. Frenkel and M. Feder, "Recursive expectation-maximization algorithms (EM) for time-varying parameters with applications to multiple target tracking," *IEEE Trans. Signal Processing*, vol. 47, no. 2, pp. 306–320, Feb. 1999.
[36] K. J. Molnar and J. W. Modestino, "Application of the EM algorithm for the multitarget/multisensor tracking problem," *IEEE Trans. Signal Processing*, vol. 46, no. 1, pp. 115–129, Jan. 1998.
[37] L. R. Rabiner, "A tutorial on hidden markov models and selected applications in speech recognition," *Proc. IEEE*, vol. 77, no. 2, pp. 257–286, Feb. 1989.
[38] M. S. Arulampalam, S. Maskell, N. Gordon, and T. Clapp, "A tutorial on particle filters for online nonlinear/non-gaussian bayesian tracking," *IEEE Trans. Signal Processing*, vol. 50, no. 2, pp. 174–188, Feb. 2002.
[39] Q. Hao, "Mulitple human tracking and identification with pyroelectric sensors," Ph.D. dissertation, Duke university, Mar. 2006.
[40] (2005) The texas instrument website. [Online]. Available: http://www.ti.com/
[41] (2005) The crossbow website. [Online]. Available: http://www.xbow.com/
[42] M. Harwit and N. J. A. Soane, *Hadamard Transform Optics*. Reading, NY: Academic Press, 1979.
[43] A. Busboom, H. D. Schotten, and H. Elders-Boll, "Coded aperture imaging with multiple measurements," *J. Opt. Soc. Am. A*, vol. 14, no. 5, pp. 1058–1065, May 1997.

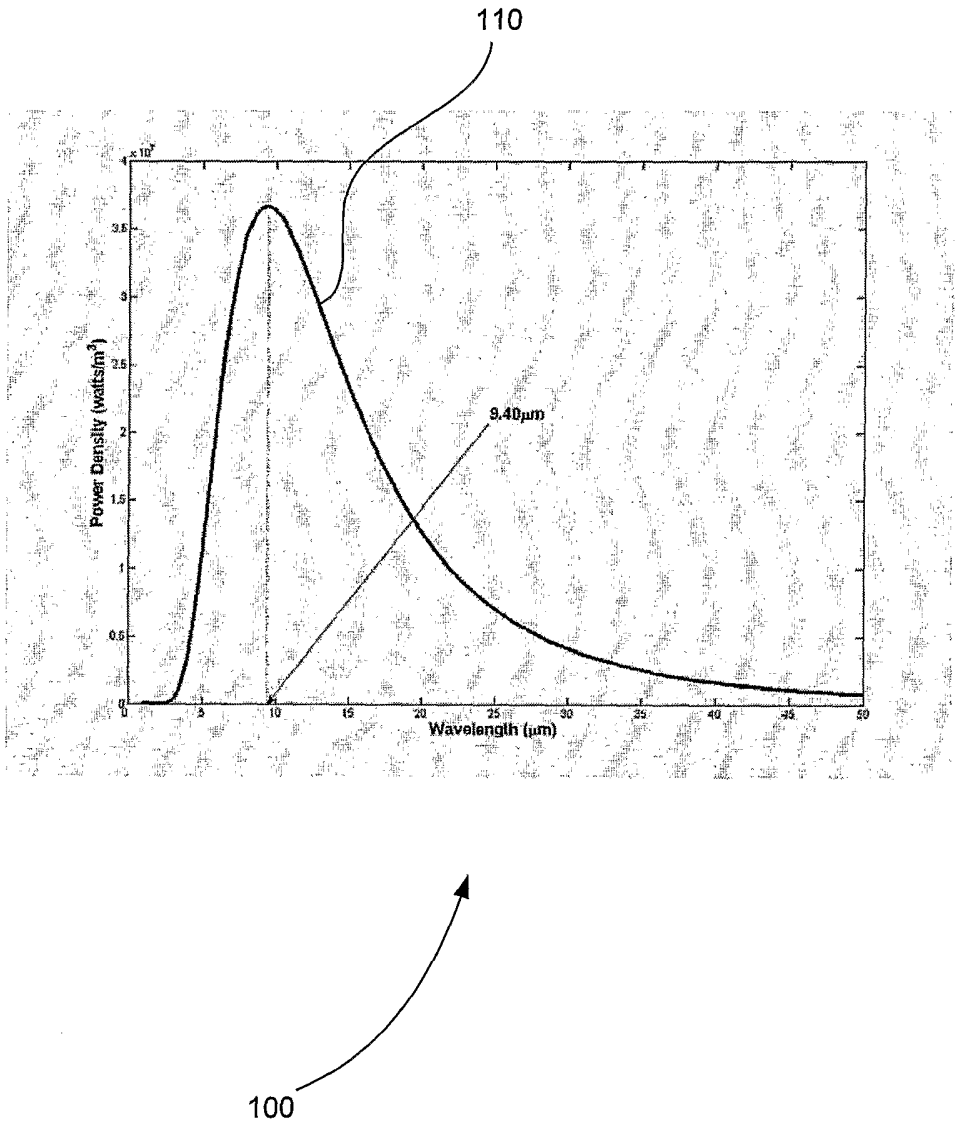

FIG. 1

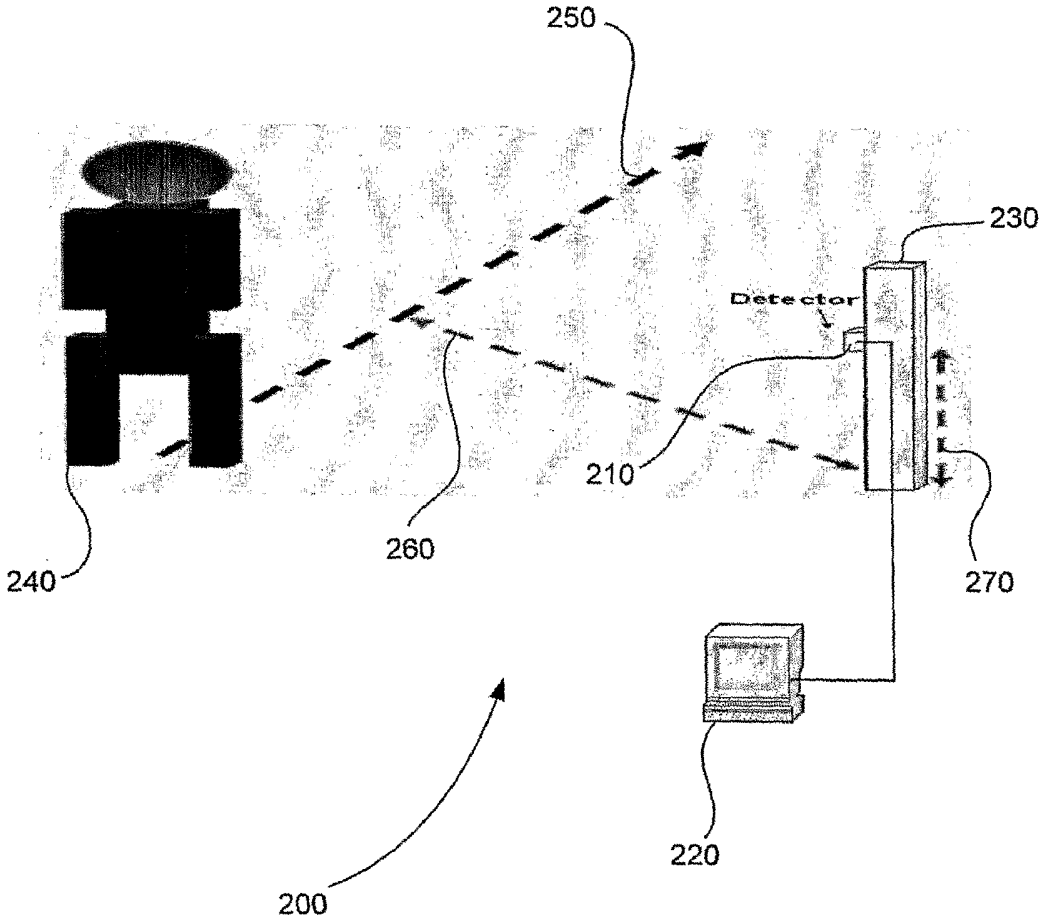

FIG. 2

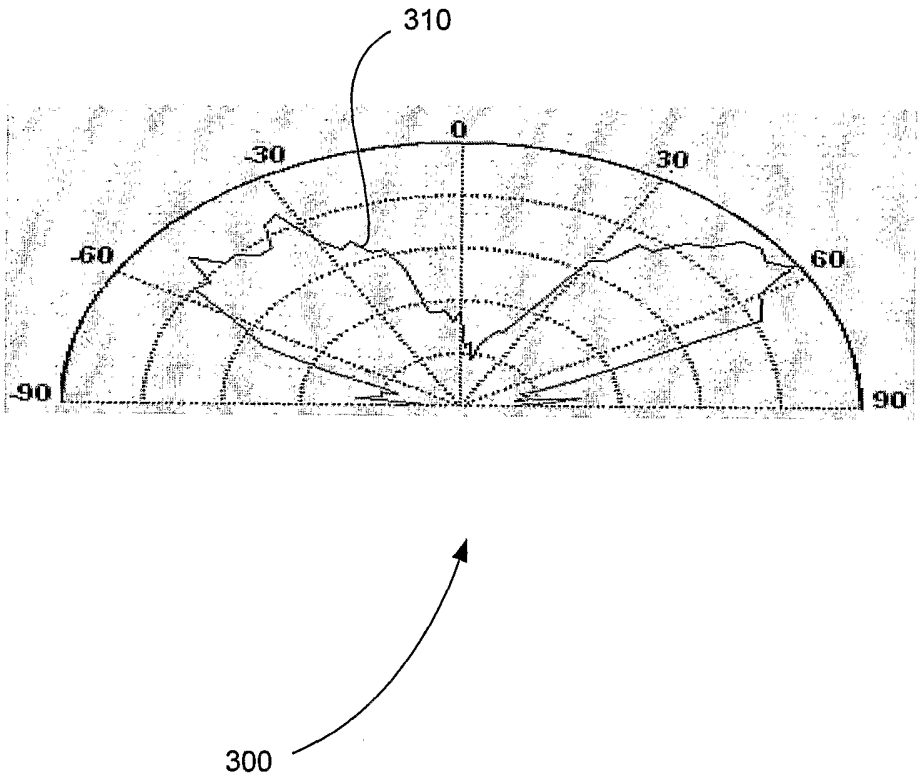

FIG. 3

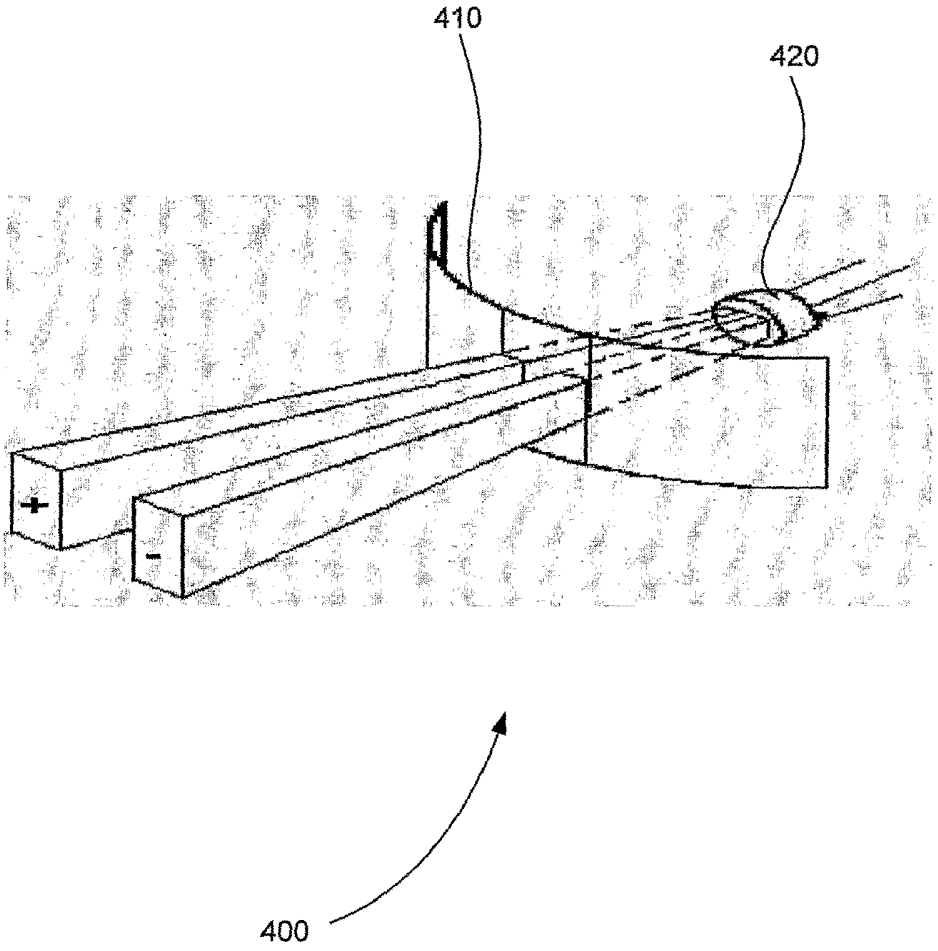

FIG. 4

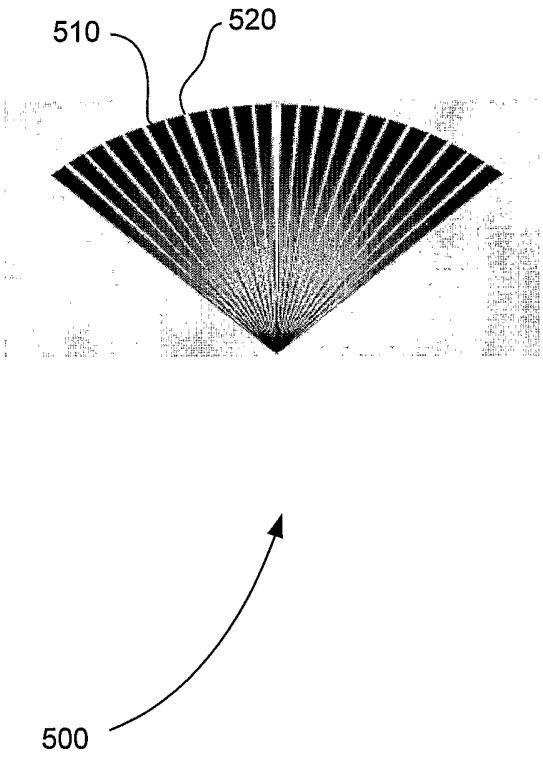

FIG. 5

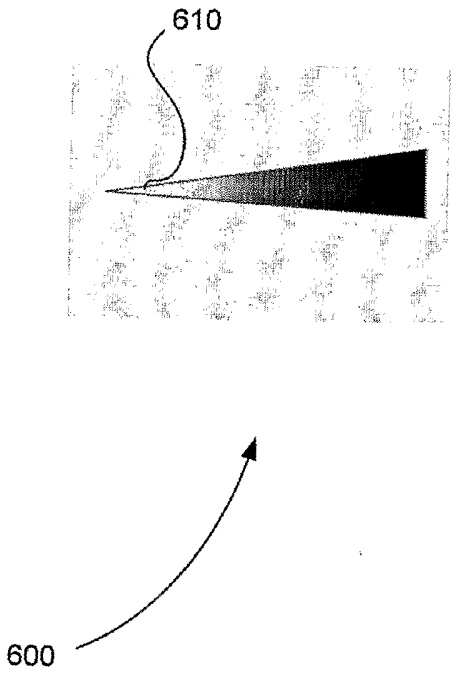

FIG. 6

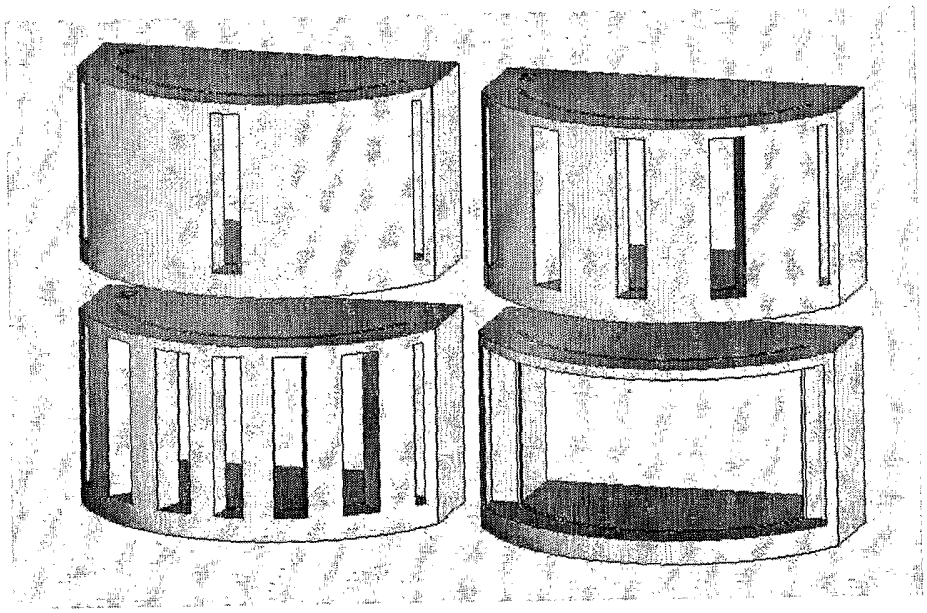

FIG. 7

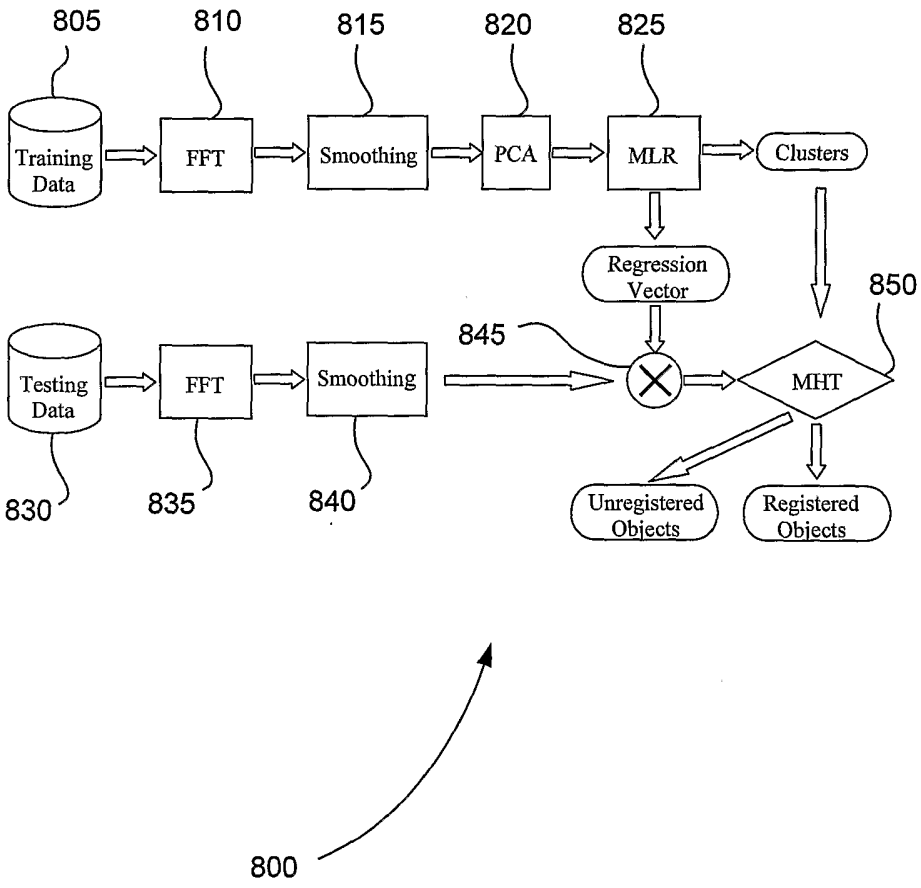
805
810
815
820
825
Training Data
FFT
Smoothing
PCA
MLR
Clusters
Regression Vector
850
845
Testing Data
FFT
Smoothing
MHT
830
835
840
Unregistered Objects
Registered Objects
800

FIG. 8

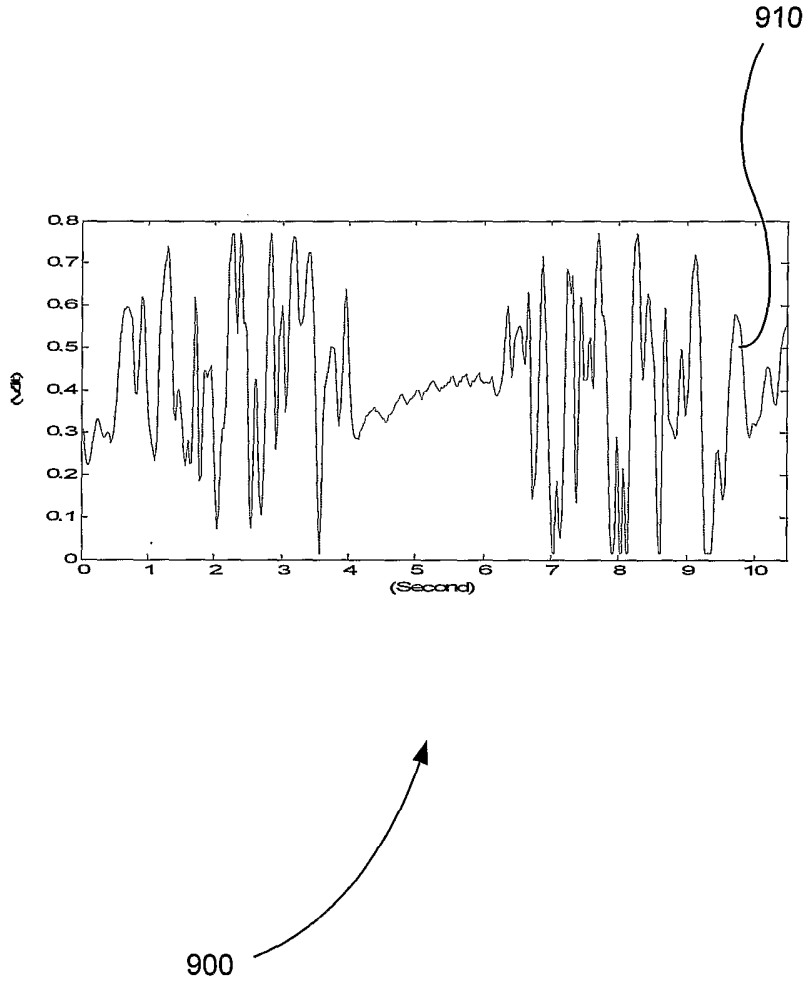

FIG. 9

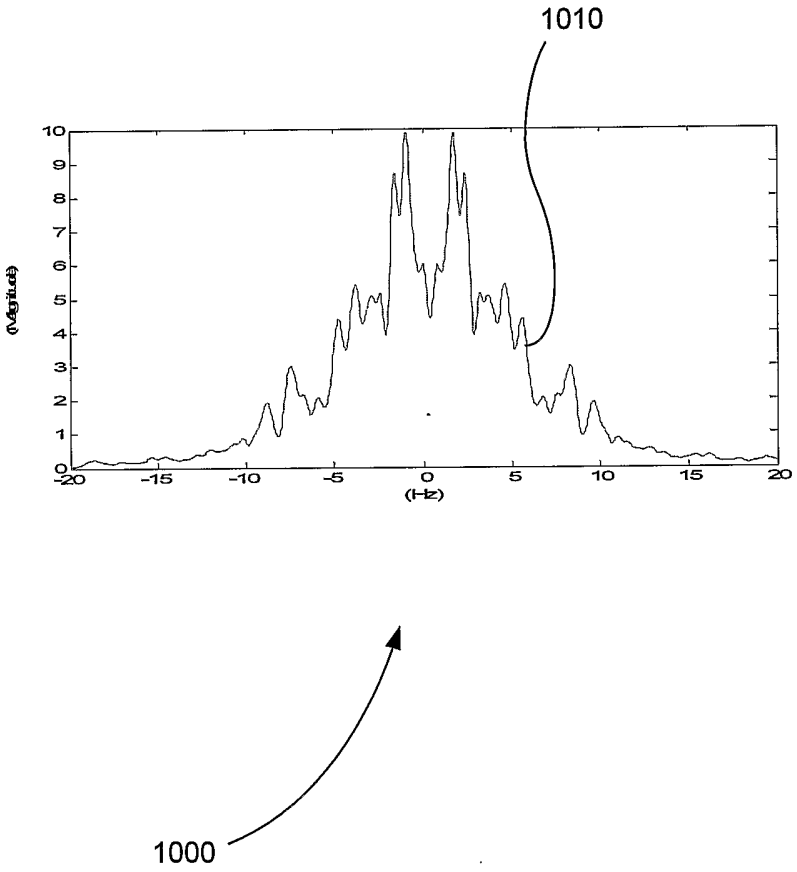

FIG. 10

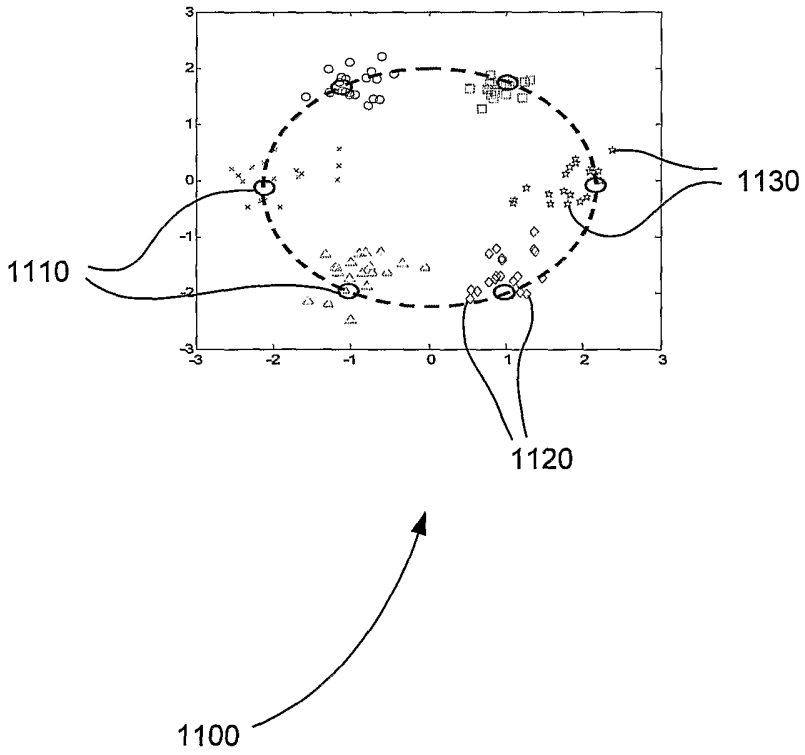

FIG. 11

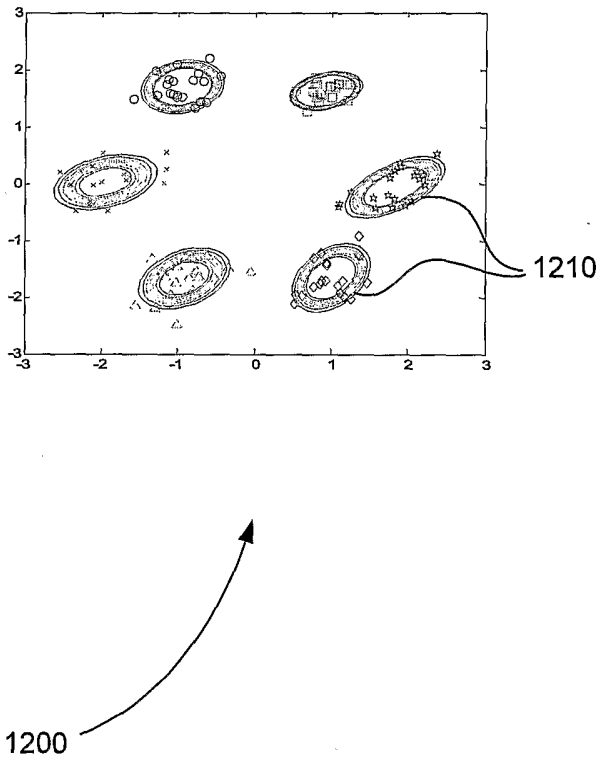

FIG. 12

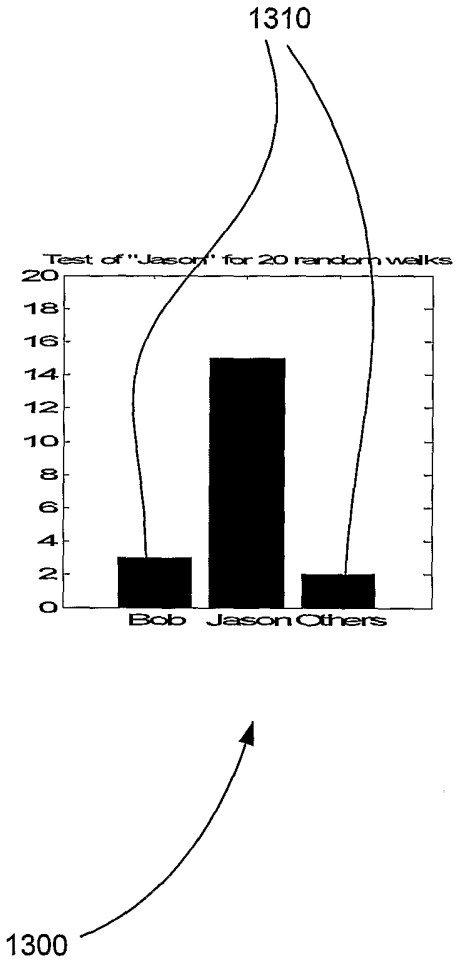
1310
Test of "Jason" for 20 random walks
20
18
16
14
12
10
8
6
4
2
0
Bob
Jason
Others
1300

FIG. 13